January 2018

Mechanisms Of Cold Region Hydrologic Changes To Recent Wetting In A Terminal Lake Basin

Diane Frances Van Hoy

Follow this and additional works at: https://commons.und.edu/theses

MECHANISMS OF COLD REGION HYDROLOGIC CHANGES TO RECENT WETTING IN

A TERMINAL LAKE BASIN

by

Diane Frances Van Hoy

Bachelor of Science, Arizona State University, 2014

A Thesis

Submitted to the Graduate Faculty

of the

University of North Dakota

in partial fulfillment of the requirements

for the degree of

Master of Science Geological Engineering

Grand Forks, North Dakota

August

2018

This thesis, submitted by Diane F. Van Hoy in partial fulfillment of the requirements for the Degree of Master of Science from the University of North Dakota, has been read by the Faculty Advisory Committee under whom the work has been done and is hereby approved.

Dr. Taufique Mahmood, Chairperson

Dr. Paul Todhunter

Dr. Philip Gerla

This thesis is being submitted by the appointed advisory committee as having met all of the requirements of the School of Graduate Studies at the University of North Dakota and is hereby approved.

Grant McGimpsey

Dean of the School of Graduate Studies

Date

PERMISSION

Title   Mechanism of Cold Region Hydrologic Changes Due to Recent Wetting in a

       Terminal Lake Basin

Department Geology and Geological Engineering

Degree   Master of Science

   In presenting this thesis in partial fulfillment of the requirements for a graduate degree from the University of North Dakota, I agree that the library of this University shall make it freely available for inspection. I further agree that permission for extensive copying for scholarly purposes may be granted by the professor who supervised my thesis work or, in his absence, by the Chairperson of the department or the dean of the School of Graduate Studies. It is understood that any copying or publication or other use of this thesis or part thereof for financial gain shall not be allowed without my written permission. It is also understood that due recognition shall be given to me and to the University of North Dakota in any scholarly use which may be made of any material in my thesis.

                      Diane Frances Van Hoy
                      May 14, 2018

TABLE OF CONTENTS

                Hydrological Response Units by Sub-Basin

                Model Setup Files

LIST OF FIGURES

LIST OF TABLES

ACKNOWLEDGMENTS

ABSTRACT

The recent changes in hydroclimatic conditions in the Northern Great Plains (NGP) have led to an increase in precipitation and wetland connectivity over the last few decades. The most recent wet period started at 2005 after the last NGP drought (1999-2004). The current wetting is expected to continue and could potentially last into 2038 and beyond. The increases in precipitation during the recent wet period yield an integrated response resulting in hydrologic changes in the NGP. However, the underlying mechanism of the hydrologic changes caused by recent wetting is poorly understood requiring a physically-based modeling framework in order to decipher them. This study utilized a field-tested and physically-based cold region hydrologic model (CRHM) to investigate the impacts of elevated precipitation on recent hydrologic changes by examining the intermediate processes during the 2004-17 period. CRHM is designed for cold regions and has modules to simulate processes, such as blowing snow transport, sublimation, interception, frozen soil infiltration, snowmelt, and subsequent streamflow generation. The modeling of the current study focuses on a tributary basin of the Devils Lake Basin (DLB) known as the Mauvais Coulee Basin (MCB). Since there were very few snow observations in the MCB, a detailed snow survey was conducted at distributed locations estimating snow depth, density, and snow water equivalent (SWE) using a prairie snow tube four times during winter of 2016-17. The MCB model was evaluated against distributed snow observations and streamflow measured at the basin outlet (USGS) for the year 2016-17. Overall, the simulated snow water equivalents (SWEs) at distributed locations and streamflow are in good agreement with observations. The simulated SWE maps exhibit large spatiotemporal

variation during the winter of 2016-17 due to spatial variability in precipitation, snow

redistribution from stubble fields to wooded areas, and snow accumulations in small depressions

across the sub-basins. The main source of snow appears to be the hills and ridges of the eastern

and western edges of the basin, while the main sink is the large flat central valleys. Snowmelt

was the primary contributor to annual streamflow with a varying contribution from rain-on-snow

(ROS). Detailed diagnosis of simulations identified two phases (pre- and post-2011) exhibiting

different cold region hydrologic responses. During the pre-2011 period, the MCB system was

dominated by both streamflow and evapotranspiration (ET) while there was extreme ET

dominance with very minor influence from streamflow in the post-2011 period. This switch was

caused primarily by climatic conditions involving spring/summer rainfall and daytime overcast

conditions. Both snowmelt and ROS contributed to annual streamflow in the pre-2011 period

while only snowmelt was the prime contributor in the post-2011 period except in 2013. Frozen

soil and basal ice conditions during the spring period played a significant role for generating

streamflow within the pre-, during, and post-2011 period.

CHAPTER I
INTRODUCTION

The Northern Great Plains (NGP) is an vital agricultural region producing a considerable fraction of the world's corn, wheat, and barley. Since, the economy of the region is dominated by agricultural practices, climate, and its variability are of scientific and socioeconomic interest. Over the last four decades, the NGP has experienced highly variable climatic regimes as it has for the past two millennia, resulting in a series of extreme dry and wet periods (Todhunter, 2016; Shapley, et al. 2005). During the extreme wet periods, the increase in precipitation, rainfall rate, and wetlands connectivity yield an integrated response resulting in high peak streamflow and subsequent flooding. In contrast, dry periods result in devastating droughts (Bonsal et al., 2011, 2013; Todhunter & Fietzek-DeVries, 2016; Todhunter, 2016; Mahmood et al., 2017). An approximately twenty-year cycle of drought has been recognized over the years with recent dry periods: 1958-62, 1983-89, and 1999-2005 (Bonsal et al., 2013; Sweeney, 1985; Weakly, 1943; Thomas, 1962). In between these droughts there were wet periods in the early 1970's and 1990's (Bonsal et al., 2013). The year 2005 marks the starting point of the recent wet period after the 1999-2004 prairie drought (Shook, 2016). The current wetting is expected to continue and could potentially continue into 2038 and beyond (Vecchia, 2008).

The recent climate changes via increased precipitation in the NGP hydrology are manifold, spatiotemporally variable, and scale dependent (e.g. Coles et al., 2016; Mahmood et

al., 2017; Todhunter, 2016). Recently, Ryberg et al. (2016) reported earlier snowmelt streamflow peaks in the northern part of the NGP due to recent climate change. High snowfall, along with high antecedent (fall) soil moisture content resulted in large streamflow and massive flooding in current years in many NGP basins including the Red River and Assiniboine, which had a strong contribution from spring/summer rain in 2011 (Blais et al., 2016; Stadnyk et al., 2016), South Tobacco Creek (Mahmood et al., 2017), and Devils Lake in 2009, 2011, and 2013. In addition to snowmelt induced runoff, the rainfall contribution to streamflow is also significant but highly variable. Many studies reported increased contribution of rainfall to streamflow at smaller watersheds, such as the outlet and sub-basins of South Tobacco Creek (Mahmood et al., 2017), while rainfall contribution to streamflow is very little at a larger watershed scale (e.g. Corrivau et al., 2013) with few exceptions, such as the Smith Creek Research Basin (SCRB) (393.0 km^2) (Dumanski et al., 2015). In a few cases, there have been rainfall only induced floods including the 2005 flood of the Saskatchewan River Basin (Shook 2016) and the 2014 flood in the Assiniboine River Basin and the SCRB (Ahmari et.al, 2016; Dumaski et al., 2015). However, streamflow is not always responsive to elevated precipitation. For example, during 2007 and 2008, the annual streamflow was very low (<10.0 mm) compared to annual precipitation (> 500.0 mm) (Mahmood et al., 2017). Although, there is a consensus in the literature of last two decades on the trends of rising spring precipitation across the various watersheds in the NGP, the shift in mean annual and winter temperature is inconsistent and inconclusive. The contemporary wetting, therefore, inevitably exerts robust control on processes in the NGP hydrological cycle with cascading influences on the streamflow generation mechanisms.

Despite many recent investigations (Kharel et al., 2016; Rasouli et al., 2014; Mahmood et al., 2017; Dumanksi et al., 2015; Bonsal et al., 2017), the mechanisms of cold hydrologic

2

changes (e.g. changes in snow processes, streamflow generation, and summer ET) to current wetting are poorly understood primarily in a cold-region terminal lake basin, such as Devils Lake basin. Thus, a physically-based modeling framework is needed to detect the impacts of recent wetting on cold region hydrologic responses. In this study, I hypothesize that the current knowledge gap in the mechanisms of hydrologic changes to recent wetting can be filled by examining changes in intermediate processes:

- snow accumulation

- snow redistribution

- blowing snow transport

- in-transit sublimation

- frozen soil infiltration

- highly seasonal ET

- streamflow generation of different origins such as:

  - snowmelt

  - rain-on-snow,

  - rainfall-induced.

Detecting the changes in intermediate processes to elevated precipitation in a comprehensive manner using field-based observations is challenging due to the need for high-resolution spatiotemporal observations over a long period. A physically-based distributed cold region hydrologic model tested adequately against field observations can be a useful tool to reproduce spatiotemporally varying hydrologic responses and detect the causal mechanisms of hydrologic changes. Physically-based distributed models have been available for decades, but have become

increasingly popular in recent years due to the wide availability of high-resolution spatial data and improvements in computer technology (Sivapalan, 2018). In the cold NGP region, the hydrologic cycle is typically dominated by wind redistribution of the seasonal snowpack, on-ground and in-transit sublimation, spring snowmelt, infiltration into frozen, partially frozen and unfrozen cultivated and tilled soils, fill and spill induced variable contributing areas and their influences on a large volume of runoff generation, depressional storage dynamics, spring and summer rainfall intensity and their spatial extents, seasonal ET, and spring streamflow. I believe that the Cold Region Hydrological Model (CRHM) is an appropriate simulator for this study as the CRHM was specially designed to model governing hydrologic processes in the cold NGP and Canadian Prairie Region. It is an object-oriented, multi-physics, and multi-modular modeling system that allows development of hydrological models representing key hydrological processes from a range of possible configurations and algorithm choices. CRHM has been extensively tested for agricultural areas in the Canadian Prairies (Mahmood et al., 2017) that are similar to the cold prairie landscape in the NGP as well as more mountainous regions, such as the Pyrenees, and the Canadian Rockies (Mahmood et al., 2017; López-Moreno et al., 2013; Fang et al., 2013).

The objective of this study is to compile a physically-based model to examine how these recent changes in precipitation influence the intermediate cold region hydrological processes and how those processes impact streamflow in a headwater basin (Mauvais Coulee Basin) contributing to Devils Lake. In particular, we inspect the emerging spatiotemporal patterns in SWE accumulations and runoff generation mechanisms as well as basin-scale mass balance for identifying underlying processes and land surface conditions responsible for recent changes in hydrology. Previous studies in the Devils Lake Basin areas (Kharel et al., 2016; Lim et al., 2010;

4

Munna, 2012; Zhang, 2010; Melesse et al., 2006; Todhunter, 2016; Ryan & Wiche, 1988) were conducted with empirical models lacking comprehensive representations of cold region processes and the temporal extent of these studies were limited to 2011. The hydrologic insights obtained from this study are germane to other prairie regions, such as the Pampa in South America, the Plains of Hungary, Romania, and historic Yugoslavia, the Manchurian Plains, and the Black Earth Belt of Russia (Grassland, 2018). The study site is an agricultural area with a minor contribution from prairie grassland and sparse forest cover. Investigating the mechanism of hydrologic change in a high-latitude agricultural basin is of hydroclimatic importance, since these areas are vulnerable to climate change. This investigation is expected to show the temporal evolution of major cold region processes occurring in the latest wet period and provide guidance to future field investigations and watershed simulations.

CHAPTER II

STUDY AREA

The study site is the Mauvais Coulee Basin (MCB) (~1032.0 km^2), which is a cold

region, high-latitude, semiarid, agricultural, low relief headwater catchment of Devils Lake. Note

that the Devils Lake Basin (DLB) itself is a sub-basin of the Red River of the North Basin, which

is a transboundary watershed (crosses the Canadian Border) in the western part of the NGP. The

MCB is located in north-central North Dakota covering parts of Rolette, Towner, and Cavalier

counties and ultimately drains to Lake Irvine (Figure 1). The highest point in the MCB is 673.2

m on the eastern edge of Turtle Mountain (northwest corner of the MCB) while the lowest point

is 442.4 m near the outlet of the MCB (Figure 1). In general, the terrain slopes from north to

south with a relief of ~230.0 m and an average elevation of ~550.0 m (Figure 1). The bedrock is

from the Cretaceous period and primarily consists of Pierre Shale, with the Fox Hill Formation in

the northwest corner (Bluemle, 2003). Glaciers created most of the surface geology and

topography of the MCB during the last glacial maximum in the late Wisconsinan (Bluemle,

2005). These glaciers left in their wake moraines, eskers, kames, and a myriad of potholes (Pusc,

1993). The region also has sand and gravel lenses, outwash deposits, lake deposits, and glacial

drift with grain sizes ranging from clay all the way up to boulders (Pusc, 1993). The MCB lies

within the Northern Glaciated Plains ecoregion covering parts of the Turtle Mountain, Northern

Black Prairie, Glacial Lake Basins, and Drift Plains sub-regions (U.S. Environmental Protection

Agency et al., 1998). In the MCB, there is a wide range of land covers that include agricultural

6

lands, hay/pasture areas, forest, grasslands, development, and wetlands (Figure 2; Multi-Resolution Land Characteristics Consortium, 2006). Turtle Mountain is heavily forested with aspen, black poplar, ash, birch, box elder, elm, and bur oak (Figure 2; Bluemle, 2005). There are also small patches of coniferous and deciduous trees in shelter belts along the edges of farms. The majority of the remainder of the basin except in the central and southern portions is agricultural lands producing a variety of crops, such as soybeans, wheat, barley, canola, sunflowers, corn, and beans (Figure 2; Natural Resources Conservation Service, 2007). The center of the basin has large areas that are classified as hay/pasture while the south-central part of the basin is predominately occupied by herbaceous vegetation (meaning native vegetation other than trees) (Figure 2). Small wetlands with a mixture of grass and cattails are dispersed throughout the basin and are increasing in size and number during the recent wet period (Figure 2; Todhunter & Rundquist, 2008). Roads of various quality some paved and some simply compacted dirt crisscross the basin (Figure 2). The primary soil type in the north-east and north-west sides of the basin is loam (a mixture of clay, sand, and silt), which is dark brown in color with a fine texture (Soil Survey Staff, 2016). The southern tip of the basin is a coarser loam and fine silt, and the center of the basin is mixture of sand, coarse and fine loam, and loam covered sand (Soil Survey Staff, 2016).

The DLB region has been classified as a cold dry continental climate in accordance with the Thornthwaite climate classification system (Todhunter & Fietzek-DeVries, 2016). Mean annual precipitation during 1951-1980, 1981-2010, 2010-17 period were 466, 579, ~518 mm respectively (Todhunter, 2016). Precipitation often fluctuates from year to year and is highly seasonal. Based on the average snowfall and rainfall for 2004-17 seasonal patterns can be found for individual water years. Water years for this study are defined as starting the second hour of

September 30 for one year and ending on the first hour of September 30 of the following year. This is based on how the simulation periods are run in CRHM. Similar to Mahmood et al. (2017) 2004-05 was a water year with a wet winter and wet summer, as were 2012-13, and 2013-14; 2005-06, 2008-09, 2010-11 were wet winters followed by dry summers; 2006-07, 2007-08, 2011-12, and 2016-17 were dry winters followed by dry summers; 2009-10, 2014-15, and 2015-16 were dry winters followed by wet summers (Table 1). Note that the winter precipitation of 2004-05 was only slightly above average as was the summer of 2007. Mean temperature during 2004-17 period at Cando, ND is 4.0°C showing a slight increase during the study period. The average winter and summer temperatures are -9.0°C and 13.0°C respectively exhibiting strong seasonality within a year. Average annual streamflow from the gage is 43.1 mm and in most years is dominated by spring snow-melt in late March to mid-April. Similar to precipitation streamflow is also highly variable and the two are often but not always, strongly correlated. Due to low permeability of the soils, the base flow contribution is very small in the basin as it was in studies for Devils Lake (Wiche & Pusc 1994; Vecchia 2002, 2008). Frozen soil and stream conditions persist for most of the winter into the spring snowmelt period.

Table 1. Weather and Streamflow for Study Area.

Year	T_{WY} (mm)	P_{WY} (mm)	Rainfall (mm)	Snowfall (mm)	Q_{WY} (mm)
2004-05	4	567	451	117	50
2005-06	6	400	269	130	73
2006-07	4	428	361	67	10
2007-08	3	491	407	84	1
2008-09	2	537	365	172	85
2009-10	4	683	578	105	38
2010-11	3	547	384	163	122
2011-12	6	301	243	57	3
2012-13	2	681	500	181	60
2013-14	2	587	447	140	21

Table 1. con.

Year	T_{WY} (mm)	P_{WY} (mm)	Rainfall (mm)	Snowfall (mm)	Q_{WY} (mm)
2014-15	4	499	431	68	6
2015-16	6	592	519	73	25
2016-17	5	419	317	102	66
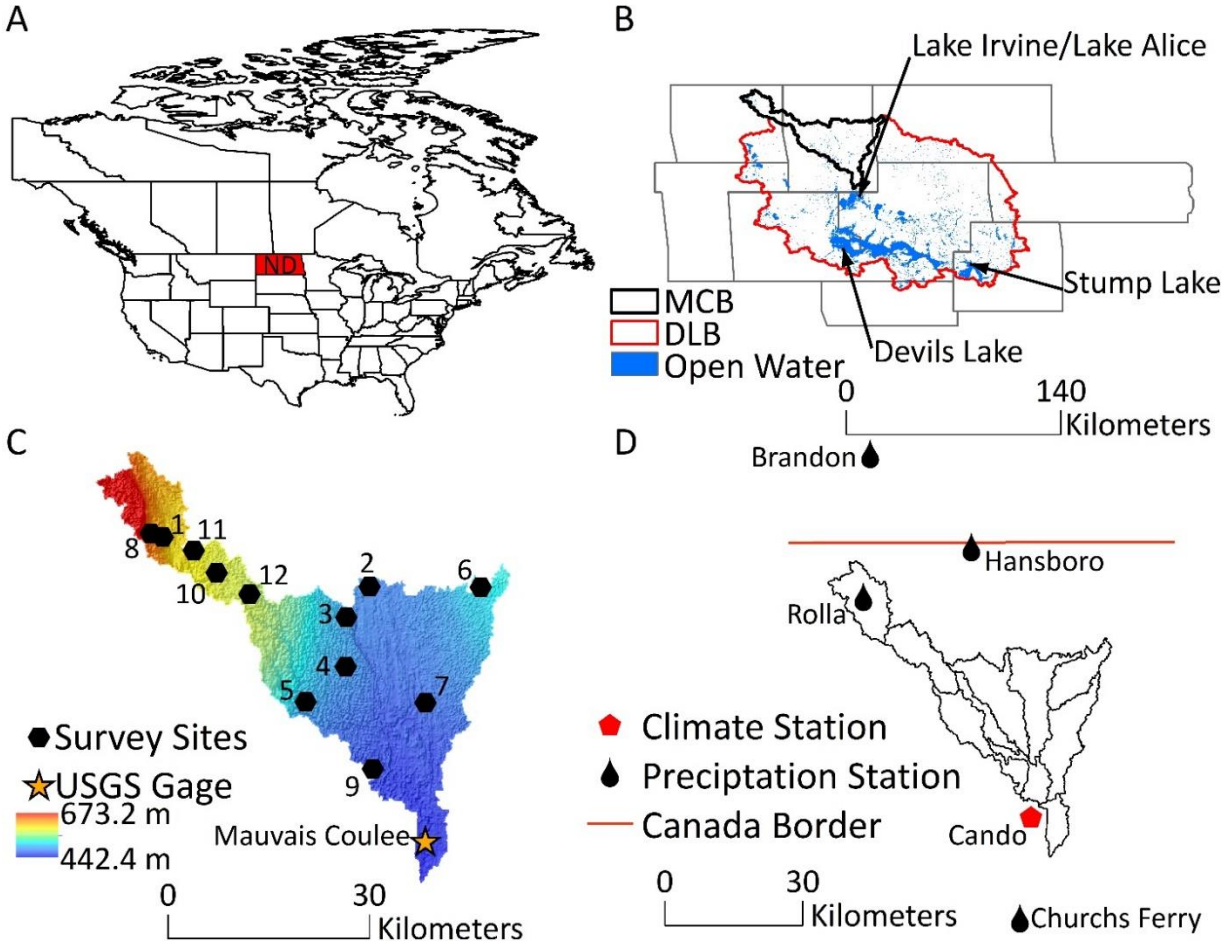
Figure 1. Study Site Location. A: Location of North Dakota in North America B: North Dakota showing the counties (grey), Devils Lake Basin (red), and Mauvais Coulee Basin (black) boundaries. C: Mauvais Coulee LiDAR Digital Elevation Model (DEM) in meters over hill shade with snow survey locations (numbered blacked hexagons) and the Mauvais Coulee streamflow gage. D: Precipitation and climate stations with the Canadian Border. Note Cando is a climate and precipitation station.
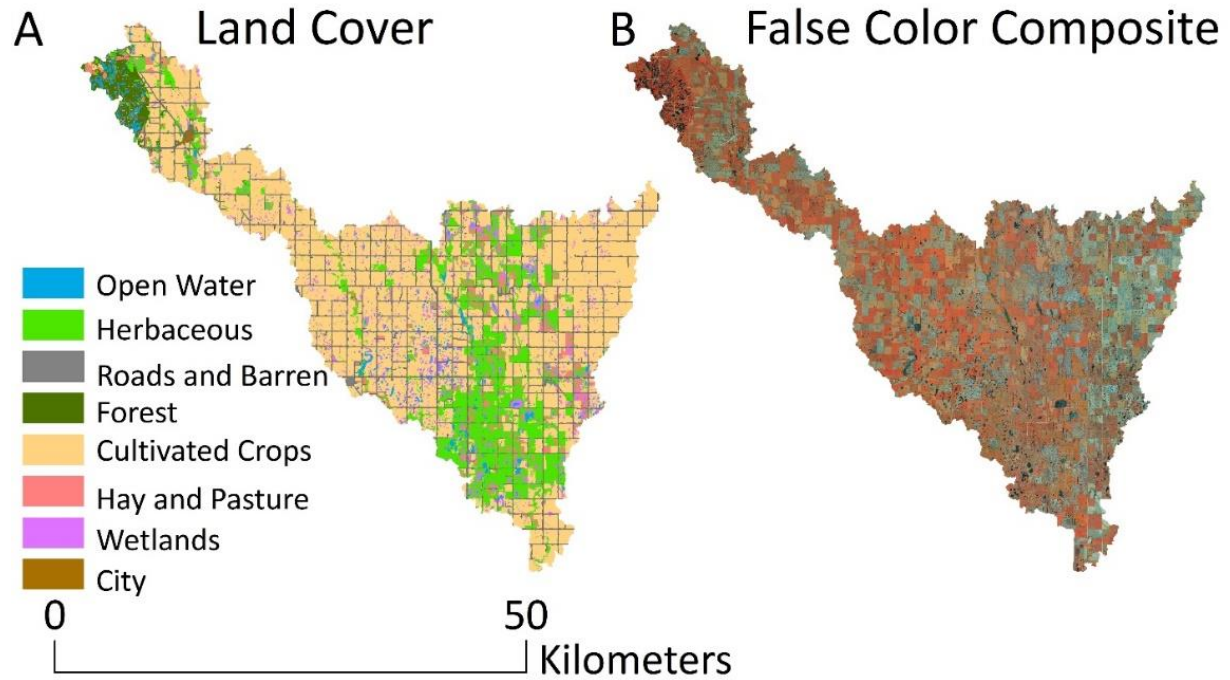
Figure 2. Land Cover of Mauvais Coulee. A: Land cover based on National Land Cover Database Map from the Multi-Resolution Land Characteristics Consortium. B: False color composite using near infrared as red, red as green, and green as blue. Red areas have a high concentration of green vegetation. Blue areas are mostly bare soil with little to no vegetation or water.

CHAPTER III

METHODS

Given the scarcity or complete lack of high-resolution ground-based measurements for hydrological factors, such as actual ET, sublimation, snow redistribution, snow accumulation, depressional storage, soil moisture, etc. the only feasible method to study the recent wet period is to create a model. This model needs to be an accurate representation of the basin in order to be a useful tool to test the hypothesis for this study. Modeling is a process that involves several steps. The first of these is to collect climate data to drive the model, SWE and streamflow data to evaluate model performance, and land surface properties to create the spatial framework of the model. The next step is to determine what processes are significant in the study area and the model modules that are needed to represent these processes. Hydrological response units (HRUs) then need to be delineated to finish the model setup. Once the data has been collected and the model setup has been created the model parameters need to be set. Finally, the model needs to be evaluated against available data to ensure that parameters are realistic. When the model has the desired accuracy it can be run to determine the various hydrological fluxes and conditions, such as ET, blowing snow, sublimation, infiltration, runoff, frozen soil, rain-on-snow, etc. that have an impact on streamflow generation.

Data Collection

Climate data including wind speed, relative humidity, incoming solar radiation, and average temperature at an hourly time step was taken from the NDAWN station at Cando. Wind speed is measured with an anemometer 3.048 m above the ground at 5.0 s increments then averaged over the course of an hour (Rithchison et al., 2018). Air temperature and relative humidity is measured 1.524 m above the ground at an interval of 60.0 s with a temperature/relative humidity sensor (Rithchison et al., 2018). Incoming solar radiation is measured every 60.0 s at a height of ~2.134 m with a pyranometer (Rithchison et al., 2018).

Spring and summer precipitation at an hourly time step are measured at the NDAWN stations at Rolla and Cando. Rain is measured to the nearest hundredth of an inch using a tipping bucket rain gage at a height of 0.914 m (Rithchison et al., 2018). These stations do not record snow between October and May. Winter precipitation data at these locations along with summer and winter precipitation for Churchs Ferry, Hansboro, and a second site near Rolla at a daily time step were taken from the Parameter Elevation Regression on Independent Slopes Model (PRISM). PRISM uses precipitation from various sources including the National Weather Service Cooperative Observer Program, Weather Bureau Army Navy Stations, National Resources Conservation Services snow telemetry (SNOTEL) and snow courses, USGS, USDA Forest Service and Bureau of Land Management Remote Automatic Weather Stations, Environment Canada, the Bureau of Reclamation Agrimet sites, the California Data Exchange Center, and various local weather stations (Daly et al., 2008). It also uses a Digital Elevation Model from the National Elevation Database (Daly et al., 2008). The model is set up around the concept that elevation is the key factor in determining spatial differences in precipitation (Daly et al., 2002, 2008). Weather stations are weighted based on clustering, distance to DEM cell,

elevation difference compared to DEM grid cell, relation to topographic features that allow for concentration of cold air, where they are in regard to terrain barriers that create orographic effects and separate air masses, areas of atmospheric temperature inversions, and coastal proximity (Daly et al., 2008). These weights are then considered in the creation of a linear climate-elevation relation for each cell in the DEM (Daly et al., 2008). While elevation differences are not significant in Mauvais Coulee it is essential to have complete precipitation data for winter. PRISM data for this study was obtained from the PRISM Climate Group, which is part of the Northwest Alliance for Computational Science and Engineering at Oregon State University. The data has a 4.0 km resolution and has under gone quality control checks (PRISM Climate Group, 2017). It is supported by the United States Department of Agriculture Risk Management Agency and has been used in many recent studies (Todhunter, 2016; Todhunter & Fietzek-DeVries, 2016; Small et al., 2006; Sankarasubramanian & Vogel, 2003). Winter precipitation data was adjusted to match various stations at Brandon, MB depending on the time period covered by that station. Brandon, Manitoba was chosen because it is close to the study site and has nearly complete and highly reliable data for the study period. Snowfall in Canada is measured using a snow ruler usually at multiple sites that are then averaged (Environment and Climate Change Canada, 2018). SWE is then found at smaller stations using the ten percent density relationship and at larger stations by melting snow that accumulates in a Nipher gage (Environment and Climate Change Canada, 2018).

Stream flow data at the outlet for Mauvais Coulee near Cando was taken from the USGS (gage: 05056100). This gage is removed from October to March due to frozen conditions in the coulee. Stage measurements at the historical gage for Mauvais Coulee were made using a stilling well on the river bank with a float that feeds data to an electronic data recorder (D. Thomas,

personal communication, 2018). When the gage was moved upstream stage measurements

started to be made using radar (D. Thomas, personal communication, 2018). Discharge is

measured at times of low flow using a SonTek Flowtracker, which makes use of the Doppler

effect to find velocity, along a transect at Mauvais Coulee (D. Thomas, personal communication,

2018). Discharge at times of high flow is measured using an Acoustic Doppler Current Profiler

attached to a floating platform, which can measure width, depth, and velocity across the coulee

simultaneously (D. Thomas, personal communication, 2018). Measurements of discharge are

taken approximately every seven weeks (C. Laveau, personal communication, 2017). Stage and

discharge are then used to develop a rating curve to interpolate discharge between measurements

(Perlman, 2016). Starting in 2009 the weir that acts as the control for low flow conditions was

inundated by backflow from Lake Alice-Irvine, and in 2012 a gage upstream of the original

started to be used for measurements (C. Laveau, personal communication, 2017). Table 2 gives

the locations of data sites in both the U.S. and Canada. Pilot Mound was only used to fill in a

one-day gap in climate data.

Table 2. Data Collection Locations.

Station Name	ID	Latitude	Longitude	Elevation (m)	Data Source
Cando 2SE		48.471903	99.166057	452.0	NDAWN
Rolla 2S		48.843	99.614	551.0	NDAWN
Rolla 1		48.843	99.614	556.0	PRISM
Rolla 2		48.9	99.6667	575.0	PRISM
Cando		48.4869	99.1976	451.0	PRISM
Churchs Ferry		48.2667	99.1833	444.0	PRISM
Hansboro		49.0	99.35	466.0	PRISM
Brandon A	5010481	49.91	99.95222	409.3	ENR
Brandon CDA	5010485	49.86667	-99.98333	362.7	ENR
Brandon RCS	5010490	49.9	99.95	409.4	ENR
Pilot Mound (AUT)	5022125	49.19103	98.90486	470.3	ENR
Mauvais Coulee Near Cando	05056100	48.45639	99.10222	440.4	USGS

Table 1 gives a summary of temperature, precipitation, and streamflow on a water year basis for the study period. Annual mean temperature was highly variable with a range of ~4.6°C during the study period with no strong overall trend. The highest average temperature was in 2011-12 (6.31°C) the lowest was in 2013-14 (1.71°C). On average warmer years (above 5.0°C) tend to have less precipitation than colder years (less than 3.5°C) with the exception of the high rainfall year of 2016. Years where the average temperature was 4.0°C ±0.5°C had a highly variable precipitation, with a range of ~255.2 mm. This may be related to the fact that this is around the temperature where precipitation changes phase. Rainfall from May to September has increased over the study period by 15.0 mm with the largest increase in the month of July (Table 3). There is no strong overall trend in snowfall although it is slightly decreasing over the study period. Streamflow also does not have any strong trend being highly variable and not always well correlated with overall yearly precipitation. Evidence for this is particularly strong in 2005-06 and 2016-17 when there is higher than average streamflow with below average precipitation, and 2009-10 and 2015-16 where the reverse is true (Table 1). The possible reasons for these and other anomalous years will be discussed later.

Table 3. Monthly Rainfall and Cloud Cover Hours

Month	Rainfall(mm)			Cloud Cover (hours)		
	Pre-2011	2011	Post-2011	Pre-2011	2011	Post-2011
May	67.0	69.0	69.0	49.0	69.0	42.0
June	98.0	76.0	104.0	55.0	57.0	30.0
July	54.0	71.0	79.0	34.0	40.0	36.0
August	73.0	44.0	49.0	66.0	32.0	51.0
September	48.0	71.0	54.0	76.0	50.0	69.0
Total	340.0	331.0	355.0	280.0	248.0	228.0

It is still highly likely that there are errors in precipitation data due to a variety of reasons including gage inaccuracy most likely caused by wind-induced undercatch. Undercatch can be

anywhere from 5.0 to 10.0% in places like North Dakota where gages have to be pole mounted to avoid being buried by snow (Shuttleworth, 2012). There may also be errors for days that were both below and above freezing most of, which were adjusted to be all rain or all snow. There may also be inaccuracies in streamflow data during the study period due to heavy vegetation, ice, beaver dams and human related obstructions (C. Laveau, personal communication, 2017).

Land surface properties must be collected in order to create and parameterize HRUs. A land cover/use map was obtained from the Multi-Resolution Land Characteristics Consortium's National Land Cover Database for 2006. This map was used because 2006 is close to the beginning of the 2004-17 study period and comparison to the 2011 study map did not show any large changes. A Digital Elevation Model (DEM) created as part of the Red River Basin Mapping Initiative of the International Water Institute was downloaded from the North Dakota State Water Commission and mosaicked in ArcGIS. The model was made using Light Detection and Ranging (LiDAR) measurements with a horizontal accuracy of a meter or less and vertical accuracy of 15.0 cm or less (Bassler, 2010). LiDAR measurements were taken during leaf-free conditions between spring of 2008 and spring of 2010 (Bassler, 2010). Soil data are from the Soil Survey Geographic Database (SSURGO) data downloaded from the Esri SSURGO downloader. SSURGO data is collected through field observations and laboratory testing by the NRCS division of the USDA (Soil Survey Staff, 2016).

Field Survey

A snow survey was conducted at ten locations across the basin for the winter of 2016-17. Most sites were chosen at random to try to create a fairly even distribution over the entire basin. All sites were located near roads to allow for ease of access. Site 8 was chosen because it was believed that the Turtle Mountain area would have a different accumulation due to the elevation

difference (Figure 1). Site 10 was chosen because it was in a wetland that had a high

accumulation in the preliminary model runs for the winter of 2016-17 (Figure 1). The survey

used the Metric Prairie Snow Sampler, which is designed after the Environment Canada ESC 30

to measure depth and a calibrated SWE scale to measure SWE (Geo Scientific Ltd.). SWE was

also calculated using a gravimetric approach to have an independent measurement for checking

the SWE scale accuracy. This SWE was in good agreement with the scale, therefore the more

numerous scale measurements were used for model evaluation. For this winter measurements

were recorded four times, on January 8, January 29, February 26, and March 26 just before the

spring snowmelt and start of streamflow.

CRHM

CRHM is a physically-based model that and has been specifically created to have the

ability to represent cold region hydrological processes through experimentally-based time tested

equations. CRHM has a flexible modular design and is spatially-distributed based on HRUs

allowing for fine scale resolution and parameterization. It has been tested in the Canadian

Prairies in many recent studies to examine drought conditions (Fang & Pomeroy, 2008; Fang &

Pomeroy, 2007), areas with a high concentration of wetlands (Fang et al., 2010) and areas

dominated by agricultural land (Cordeiro et al., 2017; Mahmood et al., 2017). The following is a

description of the modules used in this model and how they represent physical processes (Figure
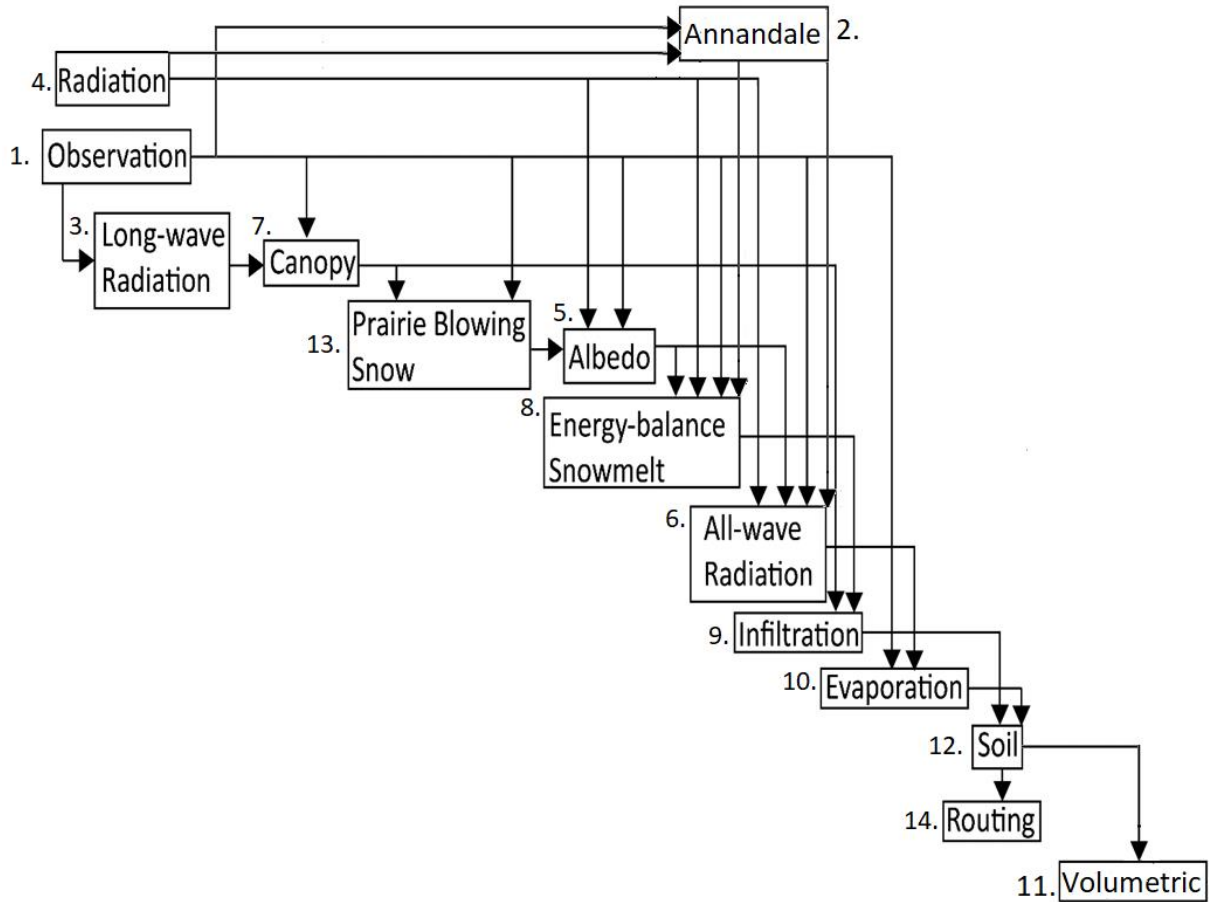
3).

Figure 3. CRHM Module Flow Chart. Numbers next to each module correspond with the descriptions below.

1. Observation Module: reads in the climate and precipitation data at an hourly time step. It was used in this model to set the precipitation, wind speed, relative humidity, air temperature, incoming longwave radiation, and incoming shortwave radiation for each HRU. Forest HRUs had the wind speed adjusted from the 3.048 m given by NDAWN to 10.0 m to account for the difference in vegetation height.

2. Annandale Module: finds the amount of radiation that is transmitted through the atmosphere based on temperature using the Annandale Method from Annandale, Jovanic, Benade, and Allen (2002) as modified by Shook & Pomeroy (2012).

18

3. Longwave Radiation Module: uses the hourly average temperature, along with relative humidity, and incoming shortwave radiation to estimate the incoming longwave radiation (Sicart et al., 2006).

4. Radiation Module: finds the direct and diffuse incoming shortwave radiation in the absence of cloud cover based on latitude, elevation, slope, and azimuth (Garnier & Ohmura, 1970). It also makes the necessary adjustments for cloud cover based on incoming shortwave radiation from the Annandale module.

5. Albedo Module: determines surface albedo in the summer based on groundcover and during the winter and spring snowmelt period based on snow (Verseghy, 1991).

6. All-wave Radiation Module: finds the net radiation during periods that are lacking snowcover using shortwave radiation, which is used to find ET (Granger &Gray, 1990).

7. Canopy Module: estimates the snow and rain that is intercepted by vegetation. It also deals with the unloading, sublimation, and melting of intercepted snow, and the evaporation and drip of collected rain. During times of snowcover the module handles the sub-canopy shortwave and longwave radiation, turbulent heat flux, and wind flux (Ellis et al., 2007, 2010; Pomeroy et al., 2009). This module is essential for finding the amount of rain and snow that reaches the ground in vegetated areas.

8. Energy-Balance Snowmelt Module: uses incoming and outing shortwave and longwave radiation to estimate the radiative, advective, convective, and internal thermal snowpack energy that is available to melt snow. Since runoff, streamflow, and to a lesser extent infiltration in spring are controlled not only by the snowmelt amount but also the rate of snowmelt it is imperative to have a module that handles this process (Pomeroy et al., 2007). This module is

based on algorithms that have been created from equations that were derived from years of observations for heat transfer (Gray & Landline, 1988; Granger & Male, 1978), net radiation (Brunt, 1932; Brutsaert, 1982; Garnier & Ohmura, 1970), and albedo (Gray & Landline, 1987; Pomeroy et al., 2007). This module has been successfully used in recent studies (Mahmood et al., 2017; Cordeiro et al., 2017; Fang et al., 2010) all of which were done in the Canadian Prairies. It is more advanced than other models because it is designed to account for differences in energy caused by slope, aspect, and changing snow albedo over time (Pomeroy et al., 2007). Snow can change albedo due to wind ablation, compaction, and mixing with soil.

9. Infiltration Module: In non-winter months this module handles unfrozen soil infiltration for rainfall based on soil properties i.e. soil thickness, soil texture, and agricultural practices, such as tillage and tile drainage (Ayers, 1959). During winter months there are three different types of soil infiltration into frozen soil restricted, limited, and unlimited. The three classes of infiltration restricted, limited, and unlimited were hypothesized to exist at the University of Saskatchewan by the Division of Hydrology (Granger et al., 1984) and have been successfully incorporated to the betterment of models in the prairies (Gray et al., 1985, 1986; Pomeroy et al., 2007).

Restricted: impermeable layers (i.e. ice lenses somewhere on or near the surface) have minimal infiltration resulting in meltwater going to runoff and ET (Pomeroy et al., 2007). If the SWE is under 5.0 mm the model will use unfrozen soil parameters (Pomeroy et al., 2007).

Limited: infiltration is dependent on snow-cover water equivalent and amount of frozen water in the first 30.0 cm of soil (Gray, Pomeroy, & Granger, 1986; Pomeroy et al., 2007). CRHM only allows for six winter snowmelt events over 5.0 mm before changing to restricted infiltration (Pomeroy et al., 2007). Melt amounts less than 5 mm infiltrates using the unfrozen

soil conditions (Pomeroy et al., 2007). When melt is above 5.0 mm the expression Melt *

Infiltration/ SWE is used to determine how much water will infiltrate; the remainder will become

runoff (Pomeroy et al., 2007). When the day after a large melt event has a temperature less than

-10.0°C infiltration is switched to restricted because the model assumes ice lens formation will

occur (Pomeroy et al., 2007).

Unlimited: Soil is heavily fractured or has large pores, so that all melt after a major

snowmelt event (> 5.0 mm) goes to infiltration (Pomeroy et al., 2007). Unlimited conditions end

when melt ends (Pomeroy et al., 2007).

The amount of infiltration is has a substantial effect on the amount of water available for

overland flow. (Pomeroy et al., 2007). The infiltration module is necessary because it is

specifically designed to handle a condition that is specific to cold regions i.e. frozen soil. Frozen

soil can effectively limit the infiltration during spring particularly in wet years (2009,2011,

2013); in dry years similar to 2007 cracks in the soil due to soil shrinkage may allow water to

infiltrate even in frozen conditions (Cordeiro et al., 2017). The equations in the module are based

on studies in Canada Prairie and Bad Lake (Gray et al., 1986; Granger et al., 1984) and what was

known as the USSR (Motovilov, 1978, 1979; Popov, 1973; Pomeroy et al., 2007).

10. Evaporation Module: utilizes the Penman-Monteith (Monteith, 1965) combination method

along with surface resistance (Jarvis, 1976) and available energy to calculate ET for most HRUs.

Other HRUs used the Priestley-Taylor method to calculate evaporation (Priestly-Taylor, 1972).

This module is necessary because evaporation has an effect on soil moisture, which in turns

affects how much water will infiltrate and how much water will become overland flow during

snowmelt or rain events.

11. Volumetric Module: finds the volumetric soil moisture based on soil properties and sets the parameter fallstat, which is the percentage of soil pore space that is occupied by water (Centre for Hydrology et al., 2016).

12. Soil Module: approximates moisture balance, slough storage, overland flow, and subsurface flow (Pomeroy et al., 2007; Dornes et al., 2008; Fang et al., 2010, 2013). Uses a three-layer approach wherein the top layer collects water from sloughs, snowmelt, and rainfall and outputs it to crops through transpiration. The second layer gets its water from the top layer of soil and also outputs water through transpiration or allows it to percolate to the third layer. The third layer is the ground water reservoir that outputs water to streams as base flow. The module ensures that ET does not exceed interception, slough storage, and "soil water withdrawal characteristics" (Mahmood et al., 2017).

13. Prairie Blowing Snow Module: calculates sublimation and blowing snow transport across HRUs using wind speed, air temperature, and relative humidity from the observation module. Snow is blown from areas of low vegetation height (i.e. low stubble) to high vegetation (i.e. higher stubble, grass, and trees) and redistribution is based on the distribution factor (Pomeroy et al., 2007). The distribution factor for all HRUs except the HRU in a sub-basin with the lowest vegetation and the highest vegetation distributes snow based on the expression a*D/ (a + b + c) (Centre for Hydrology et al., 2016). In this expression D is the amount of transport and a, b, and c are the distribution factors from HRUs A, B, and C (Centre for Hydrology et al., 2016). If the distribution factor is negative the HRU is filled to its capacity based on vegetation height. For the HRU with the lowest vegetation the snow transported out of the HRU is transported into the rest of the sub-basin based on the expression D [HRU 1] *Drift [HRU 1] (Centre for Hydrology et

al., 2016). For the HRU with the highest vegetation drift out of the HRU depends on the value of

the distribution factor as follows (Centre for Hydrology et al., 2016):

- Distribution factor > 0 snow in excess of what can be trapped by vegetation goes

  completely out of the sub-basin.

- Distribution factor < 0 all drift is trapped within the HRU.

- Distribution factor $= 0$ all drift goes out of the sub-basin.

Windy conditions occur on almost a daily basis in the NGP, due in part to the fact that there are

no natural wind breaks as there are in mountainous regions, such as the Rockies, Alps or Andes.

Therefore, blowing snow especially in high accumulation years similar to 2009, 2011, 2013, is a

noticeable component of the hydrological mass balance that needs to be incorporated into any

model for the NGP. Blowing snow results in two modes of transportation saltation and

suspension. When the snow particles are suspended they have maximum exposure to air, and can

easily sublimate accounting for as much as 15.0 to 41.0% of snowfall (Pomeroy et al., 2007;

Pomeroy & Gray, 1995). Blowing snow creates larger differences in SWE in areas of varying

land cover (Pomeroy et al., 2007; Gray et al., 1979).

14. Routing: routes water using the Muskingum routing method from HRUs to down gradient

HRUs or to the sub-basin outlets and then from the sub-basin outlets to the basin outlet at the

lowest elevation in the model (Mahmood et al., 2017). In this study flow was routed from an

HRU to the nearest stream HRU. All small streams were then routed to the main stream (Figure

4). This module is critical because it controls where overland is directed. Overland flow is the

largest contributor to stream flow hydrographs during intense precipitation events. It will also

become more important if sloughs start to connect in the basin due to the fill spill mechanism
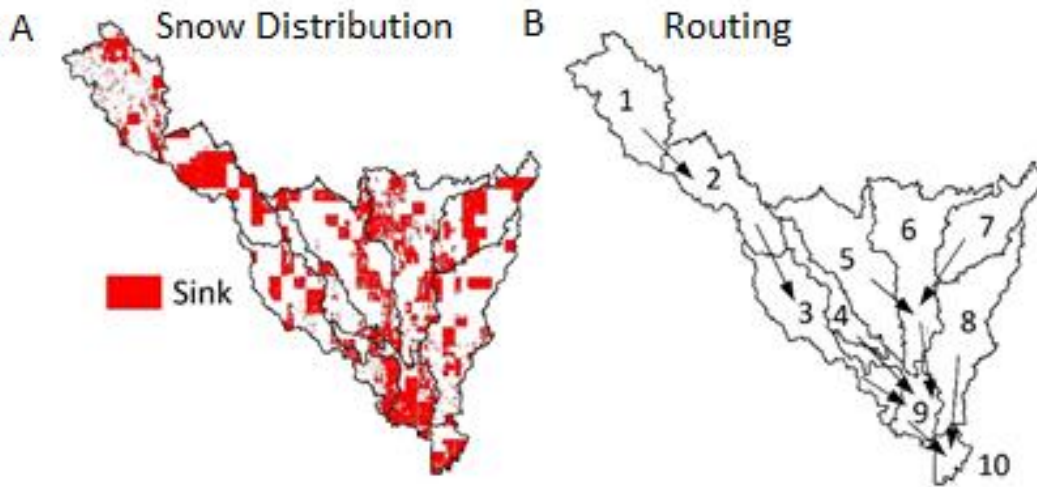
Figure 4. Model Setup. A: Snow distribution with sinks shown in red. Sinks are delineated as areas that have a negative distribution factor. B: Map of sub-basins with arrows showing streamflow routing.

HRUs

HRU Development

The MCB has been previously separated into ten sub-basins by the U.S. Geological Survey, which for the model were further divided into 498.0 HRUs (Figure 4). The shape of sub-basin 10 of the MCB was modified to account for the fact that the streamflow gage has been moved since the shape of the watershed was first delineated the USGS. This was done by finding culverts in aerial images, burning those culverts into the DEM, then running the ArcMap hydrology tools Fill, Flow Direction, Flow Accumulation, and Watershed. In the model each sub-basin has the same setup of modules to represent hydrological processes including infiltration, evaporation, blowing snow redistribution, snowmelt, streamflow routing, etc. In the MCB there is very little change in elevation with an overall relief of 230.8 m with the highest relief of ~ 127.4 m in sub-basin 1, which has an area of ~124.8 km^2. The highest slope is ~0.035 and there is also almost no difference in aspect. The soil in most of the MCB is some form of

fine textured loam. Therefore, it is believed that neither slope, aspect, or soil play a chief role in hydrological differences throughout the basin, which leaves elevation and vegetation. Vegetation was based on the NLCD map from 2006, and elevation was based on the DEM from the NDSWC. The NLCD has categories for deciduous forest, evergreen forest, herbaceous, herbaceous wetlands, woody wetlands, barren land, low, medium, and high-intensity development, cultivated crops, hay/pasture, and open water bodies (Figure 2). The deciduous and evergreen forest categories were combined into one forest classification and the woody and herbaceous wetlands were combined into one wetland classification. In areas with a high amount of forest or wetlands, such as sub-basin 1 (Figure 2) HRUs for these classifications were also separated based on elevation. Cultivated crops and hay pasture lands were typically separated based on roads, which based on field observations act as a barrier to snow redistribution predominantly in areas with roadside ditches. High/medium intensity development coincided with the city of Rolla and were combined. Low intensity and barren categories were put together to form the classification labeled in the land cover map as road and barren. Streams in the USGS's National Hydrography Dataset were made into HRUs based on stream connectivity. Maps of HRUs for each sub-basin are in Appendix A. Areas where streams overlapped open water bodies were subtracted from the streams. Routing of the sub-basins for streamflow is as follows sub-basin one drains into 2; 2 into 3; 5 and 7 into 6; 3, 4 and 6 into 9; and finally 8 and 9 into 10 where the gage is located (Figure 4).

HRU Parameterization

HRUs were parameterized for slope in ArcMap by finding the highest point the lowest point and the distance between them. The distribution parameter for drift was determined by

25

finding the elevation at the center and the four edges of each HRU. HRUs that were higher in the

middle were given positive distribution values and HRUs that were lower in the middle were

given negative distribution values. Soil texture and type was based on the soil type that covered

the majority of the HRU. Vegetation parameters leaf area index (LAI), stock area, number of

stocks per square meter, and vegetation height are rough estimates based on the vegetation type

from the land cover/use map. These parameters were adjusted to obtain a better total streamflow

volume on a yearly basis. Penman-Monteith evaporation was used except for roads, streams, and

open water bodies, which used the Priestly-Taylor method. Frozen soil area (*fsa*) is from the

CRHM parameter crack on, which is binary with 0 as unfrozen soil and 1 as frozen soil. Crack

on is set separately for each HRU, starts when the SWE is greater than 25.0 mm for the first

time, and ends when SWE is 0.0. After exporting the crack on parameter for every HRU,

equation 1 can be used to find the proportional area of frozen soil from 0 to 1.

$$fsa = \frac{\sum_{i=1}^{x} crack\ on * A_i}{A_{Total}} \hspace{3cm} [1]$$

where x is the number of HRUs in the basin.

Model Initialization and Evaluation

The climate data for September 2001 to September 2004 were used to force the model for

a run up time to set initial conditions for variables, such as depressional storage and soil

moisture. Then the model was run for September 2004-05 with subsequent years utilizing the

previous year to set the initial conditions. The model was evaluated for streamflow using the

only available gage for Mauvais Coulee, which was taken as being the outlet in the model on

both a yearly basis and for the entire test period from September 2004 to September 2017.

Streamflow is an key indicator of model performance because it is the only output flux that is

26

reliably measured in the basin. Each measurement is given a rating of either excellent, good, fair, or poor that have an accuracy of 3%, 5%, 8%, >10% respectively. The model was also evaluated against the winter of the year 2016-17 based on field survey measurements of SWE for HRUs matching the study sites. This was done to tell how well the model was capturing snow redistribution/ accumulation patterns on a basin-wide scale. Both evaluations were based on the Nash-Sutcliffe Efficiency (*NSE)* defined by equation 2 (Nash & Sutcliffe, 1970) and the relative bias (*RBIAS*) defined by equation 3.

$$NSE = 1.0 - \frac{\sum_{i=1}^{n}(x-y)^2}{\sum_{i=1}^{n}(x-\bar{x})^2} \qquad [2]$$

$$RBIAS = \frac{\sum_{i=1}^{n}(x_i-y_i)}{n*\bar{x}} \qquad [3]$$

where x is gage data, y is model output, n is the number of hours run during the simulation period, and x bar is the mean of all observations.

CHAPTER IV

RESULTS AND DISCUSSION

Snow Survey Observations

Since there are very few snow observations available in most of the study area, a snow survey was conducted over four days in the beginning of 2017. The following gives the results of that survey. Figure 5 shows the spatiotemporal distribution of SWE (Figure 5A), snow density (Figure 5B), and snow depth (Figure 5C) at distributed locations across the MCB. Overall, the observations at higher altitude in the sub-basins of the northwestern part of the MCB (Turtle Mountain) had higher snow accumulations, density, and depth than other locations throughout the 2016-17 winter season (Figure 5). Note that the higher snow accumulations at the northwestern part of the MCB are partly due to elevated precipitation in these high altitude areas (~between 550.0-600.0 m) (Figure 1). The northeastern part of the basin is also at a higher elevation than the rest of the basin (~475.0 to 500.0 m), but unlike the northwest corner does not seem to have elevated precipitation and has very little snow accumulation (Figures 1 & 5). The difference in accumulation between these two corners is likely based on others land surface factors, such as vegetation and intra-field topography. The northwest corner has the heavily forested Turtle Mountain and more herbaceous areas than the northeast corner, which is almost entirely cultivated crops (Figure 2). These herbaceous areas have taller vegetation, which tends to trap a larger accumulation of snow that is less vulnerable to midseason melting and blowing snow redistribution. Turtle Mountain also represents an area with a high density of depressions,

28

which can trap snow especially if they are dry. The north central portion of the basin is low lying and has a mixture of herbaceous and cultivated areas (Figures 1 & 2). In this area, snow accumulation is low to above average and vegetation height and density are the dominate factors controlling snow accumulations. The south central part of the basin is predominantly herbaceous with very little relief overall. This area likely has moderate to high accumulation due to the tall vegetation particularly in topographic lows. The southern tip of the basin is predominantly agricultural fields with very little relief and likely has low snow accumulation, but could be highly variable due to varying stubble height and field scale or smaller variations in topography.

Sites 1, 8, and 10 exhibited the typical pattern of overwinter snow densification over time due to compaction of snow and increasing liquid water content (Figure 5B). Site 1 is a depression with high stubble from sunflower plants. Site 8 is a low-lying field with a small amount of low stubble and a shelter belt of trees. Site 10 is a field containing a small wetland with grass and cattails. In contrast, other sites particularly 4 and 7 experienced a decrease in density that corresponds to a decrease in the depth and SWE due to snow erosion by blowing snow transport, sublimation, and midseason melting due to warm temperatures in February (Figure 5). These sites (4 and 7), being mostly bare soil with some stubble, trap less snow and tend to melt earlier in the season. Site 7 had a shelter belt where the under-canopy snowpack was sampled on the first day of the survey. This shelter belt had the highest accumulation of any location within the site due to trees trapping the blowing snow, through fall, and falling intercepted snow.
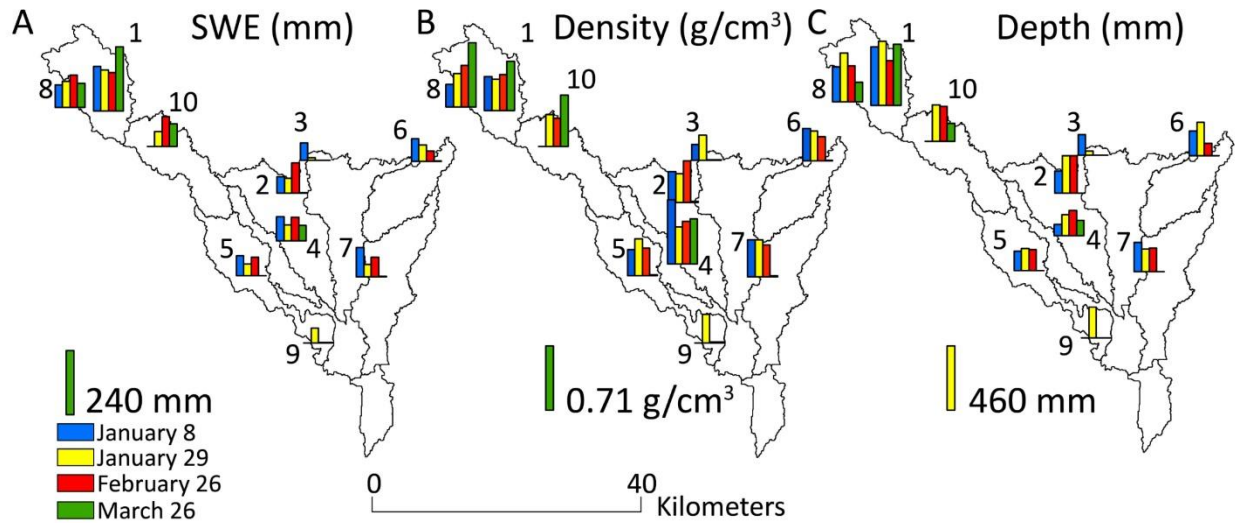
Figure 5. Snow Survey Results for the Winter of 2016-17. A: SWE (mm) measured using a snow tube and SWE scale. B: Density (g/cm^3) using volume from snow tube and mass from a scale. C: Depth (mm) measured using a snow tube. Note SWE and depth are averages from the site for the given day. Blue bars represent January 8, yellow bars are January 29, red are February 26, and green are March 26. The vertical bar in the legend of each figure represent the highest measurement overall and the numbers 1-10 represent survey locations.

The following are some visual observations that were made while collecting measurements. Snow in most of the MCB tends to accumulate in small depressions, along the banks of the coulee, and in roadside ditches. Small ponds generally freeze completely creating a low friction surface. Frequent high winds blow the snow across these surfaces, which gets trapped by surrounding wetland vegetation or roadside ditches. In areas of tall dense grass, there is little snow actually within the grass. The grass gets bent under the weight of snow, then the snow continues to accumulate overtop the flattened grass. Snow accumulates in the shelter belts but these are few and far between and do not represent a majority of the area in any sub-basin in the MCB watershed.

Overall the hummocky topography, differences in vegetation, and changes in elevation and elevated precipitation in the northwest are the primary factors that contribute to the spatially variable observed snow accumulation patterns. Figure 6 shows the SWE temporal dynamics and

subsequent snowmelt streamflow observations. The black dots represent the average of the survey measurement for each day with the bars representing ± 1.0 standard deviation. Note that the high standard deviation on March 26 is due to highly variable SWE across the MCB. At some sites, the SWE was over 200 mm (e.g. site 1) whereas only a trace amount of SWE was detected at other sites (e.g. site 2,3,5,6,7, and 9). Although, the spatially averaged SWE (~48.0 mm) on March 26 (streamflow starts at March 31) is slightly lower than the snowmelt streamflow (~56.0 mm), the spatially distributed observations using ten sites are adequate considering the spatiotemporal uncertainty in both SWE and streamflow measurements (Figure 6).
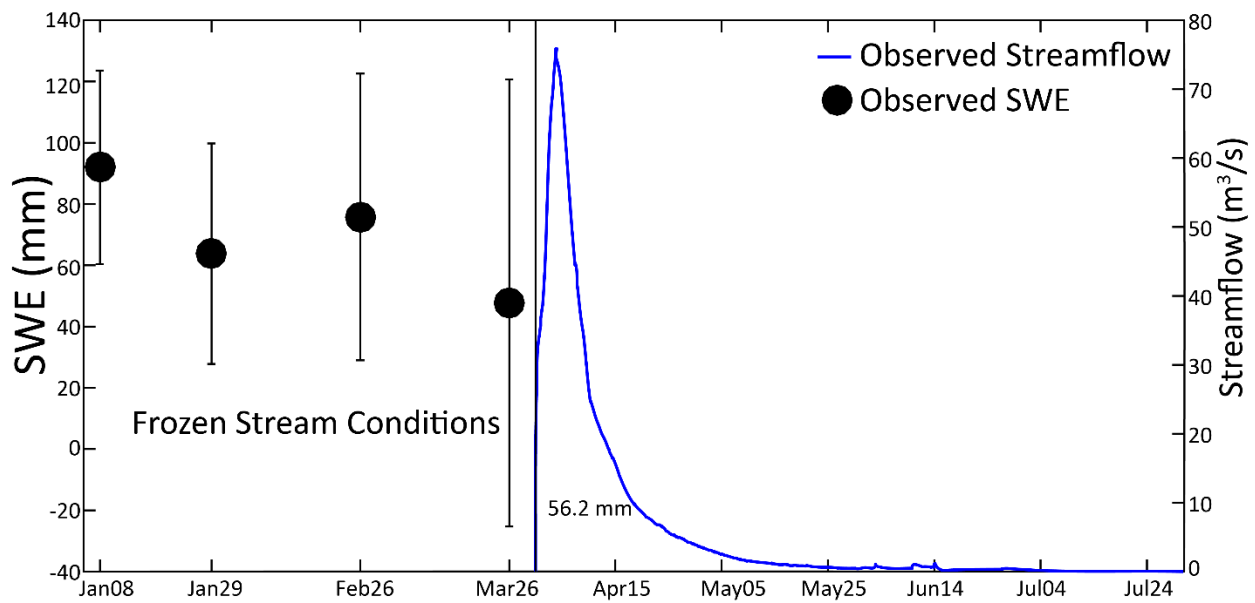

Figure 6. Hydrologic Observations for Winter of 2016-17. Black circles represent the average SWE of all survey locations on the survey days for 2017. The blue line is streamflow data from the USGS gage. The black line on March 30 represents the time when the coulee thawed.

Model Evaluation

Snow Model Evaluation

The snow model was evaluated against the distributed observations (ten sites in Figure 1) across the MCB during the winter of 2016-17. Overall the model had strong performance for all sites for the four survey days with a *NSE* of 0.7 and an *RBIAS* of 4.3%. Figure 7 shows the observed SWE (black circles), simulated SWE (blue line), and the simulated cumulative snowfall (red line) at six locations for the winter of 2016-17. In Figure 7, the vertical bars represent ± 1.0 standard deviation of the observations and the red and blue lines are HRU co-located with observation sites. A visual examination of observations and simulations shows good model performance (Figure 7). The snow model successfully reproduced the snow accumulation and intra-winter redistribution as evidenced by the fact it captured changes prior to peak SWE and that it performed adequately in capturing peak SWE at sites 1, 4, and 10 (Figure 7). The performance tends to be the better in areas where the SWE increases over the season (sites 1 and 10) than in sites where the snow melts early leaving patches of exposed soil (Figure 7). Higher accumulated snowfall than peak SWE indicates snow erosion processes (sites 3, 4, 5, 9, and 10), such as snow redistribution out of the HRU, sublimation, and melt (Figure 7). In contrast, the HRU co-located with site 1 had peak SWE substantially greater than cumulative snowfall indicating the interception of blowing snow due to the presence of a depression and high stubble height from the remnants of sunflowers (Figure 7). In the CRHM model, vegetation height, density, stalk diameter, and topography control the aerodynamic roughness, which plays a major role in blowing snow transport.
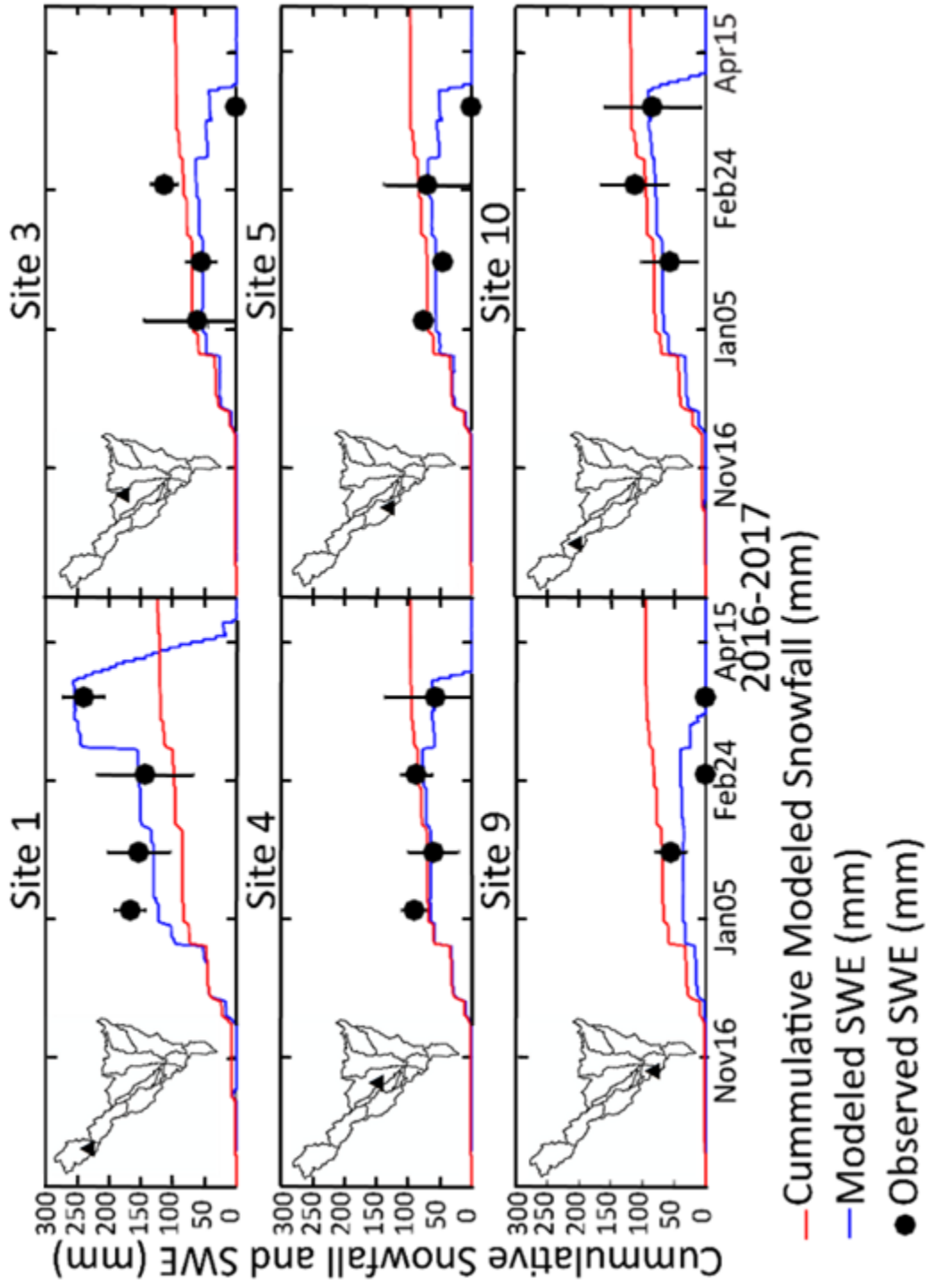
Figure 7. Snow Model Evaluation for Survey Sites. Inset maps show aerial imagery and snow survey site location. The red line is cumulative snowfall from the model. The blue line is snow water equivalent from the model and the black circles are the measured snow water equivalent with bars for one standard deviation.

The spatial modeling of snow accumulations was examined by investigating temporal changes of simulated SWE maps (Figure 8). Figure 8 also shows the comparisons between modeled SWE surfaces and field observations on the four observation dates. Overall the model captured the observed spatial patterns of SWE and was able to exhibit a wide range of spatial variation across the MCB. We restricted the upper limit of the legend of the SWE map to 125.0 mm to better reveal the emergent spatial pattern. However, for the March 26 SWE map, the maximum SWE is ~467.2 mm (Figure 8) with ~255.0 mm at site 1, which agrees with observations. The HRUs with high elevation in the northwestern and northeastern MCB show higher SWE throughout the winter of 2016-17. Turtle Mountain at the western edge of the most northwestern sub-basin (sub-basin 1 in Figure 4) provides adequate relief to create a slight orographic effect resulting in higher annual precipitation (Figure 1). Turtle Mountain is the most heavily forested part of the MCB with many small depressions that can capture snow during blowing snow transport. In contrast, the HRUs at low elevations in the center of the basin tend to have low snow accumulations. This is in part due to high winds that blow the snow out of these areas, and possibly out of the basin entirely. In addition, the basin experienced a mid-season warm period leading to erosion of the snowpack and subsequently large patches of bare soil particularly in areas where accumulation was low earlier in the season. These areas will have their peak SWE earlier in the season (December or January) unless there are large late season storms (late February to March) (Figures 5 & 8). The March 26 simulated SWE surface provides the latest status of SWE prior to melt runoff, which for 2017 was first recorded by streamflow gage on March 31. The HRUs in red in Figure 4 show the areas of snow sinks (i.e. areas with high snow accumulation). These HRUs are depressions resulting in interception of snow during blowing snow transport, very little snow erosion, and subsequent overwinter snow densification.

We believe that the snow simulation is adequately capturing SWE prior to melt runoff as basin average simulated SWE is ~61.0 mm and gaged streamflow during melt runoff (March 31 to April 20) is ~56.2 mm.
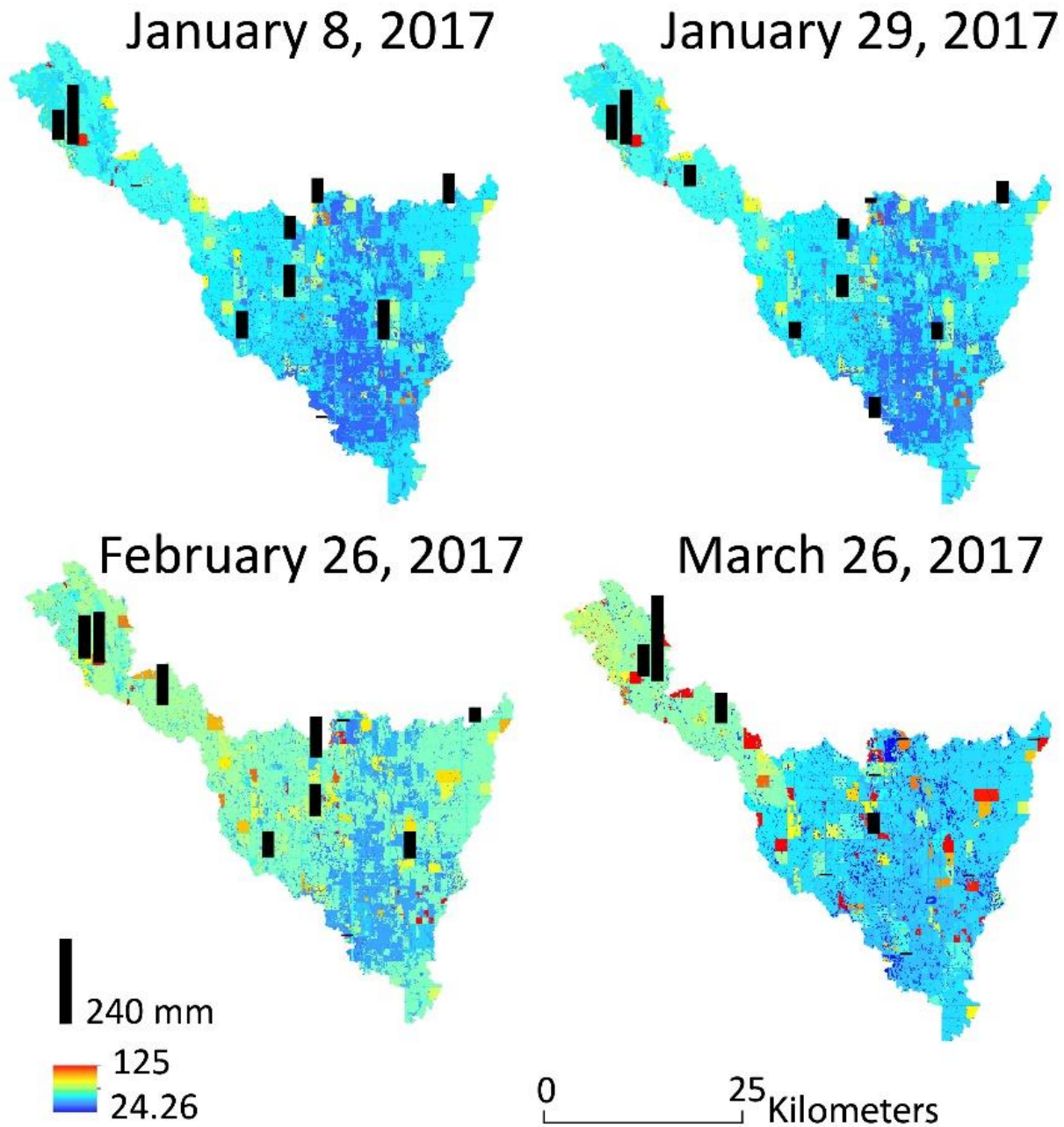
Figure 8. Comparison of Survey to Model Results for SWE in the Winter of 2016-17. Measured snow water equivalent for survey dates in 2017 shown by black bars with the maximum being 240.0 mm on March 26. The background colors are modeled SWE on the given dates for each HRU. The red areas on the maps are areas of higher accumulation due to either high vegetation presence of a depression or a combination of both.

For further analyses of 2016-17 hydrologic responses, Figure 9 shows the simulated surfaces of peak SWE (Figure 9A), time averaged SWE (Figure 9B), snowcover duration (Figure 8C), the starting time of the melt runoff (Figure 9D), and melt runoff volume (Figure 9E). As expected, the HRUs on and near Turtle Mountain show higher snow accumulation (peak SWE and time averaged SWE), longer snowcover duration, and larger slightly delayed melt runoff than the remainder of the MCB. In contrast, the HRUs at the central part of the basin yield little melt runoff due to less snow accumulation and shorter snowcover duration. Overall, the basin-wide melt starts (Figure 9D) at DOY 91 (April 1) which agrees well (± 1.0 day) with the streamflow onset time at the outlet gage.
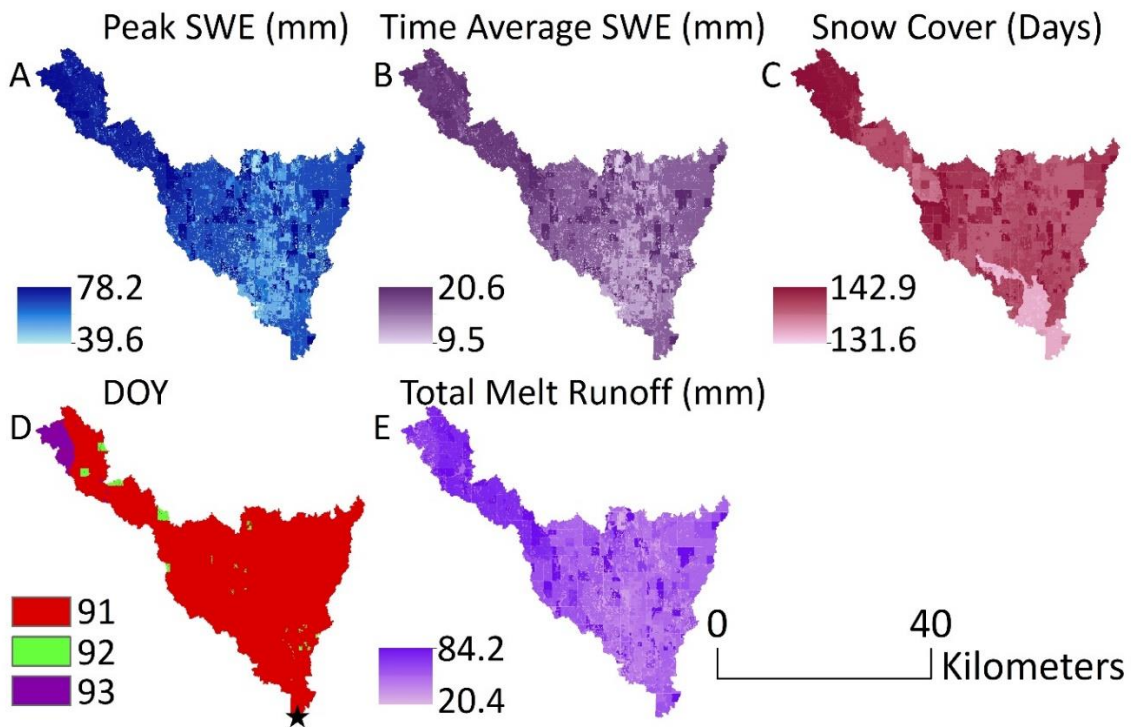
Figure 9. Model Output for 2017 by HRU. A: Peak SWE (mm) with a maximum of 468.0 and a minimum of 40.0. B: Time Average SWE (mm). C: Snowcover (Days) based on SWE being greater than zero. D: DOY stands for day of year and is the day that melt runoff starts. E: Yearly total melt runoff (mm).

Streamflow Model Evaluation

In addition to snow model evaluation with limited data (2016-17), a further model evaluation was conducted against the streamflow observations during the recent wet period (WY 2004-17). Overall, the model showed good performance while simulating streamflow. An *NSE* of 0.5 and *RBIAS* of 3.6% demonstrate the model's capability of reproducing hourly streamflow under variable hydroclimatic conditions (Figure 10). Note that the model was not calibrated but it was simulated using the parameters that provided a good match for SWE observations. There was strong model performance during hydrologically wetter years, such as 2006, 2009, 2011, 2013, and 2017 with the best performance occurring in 2005-06 and 2008-09, which both had a *NSE* of 0.75 (Figure 10). Note that, the MCB experienced local and regional flooding during these hydrologically wet years and the model was able to capture peak flow (Figure 10). However, the model performance was weaker during dry years as it overestimated the dry years of 2007-08 and 2011-12 and underestimated the dry year of 2006-07. Our model performance agrees with the study by Cordeiro et al. (2017) who used CRHM to study hydrology in Manitoba at the La Salle River from 1992 to 2013 and found that it performed best during wet years. Such discrepancies can be attributed to the inadequate spatial representation of spring and summer rainstorm events and their intensities due to lack of rain gages across the MCB. Note that there are only two rain gages in the MCB ($\sim$1032.0 km^2). It is anticipated that the hydrograph at the outlet gage could be more closely matched by modeled streamflow using calibration of land surface, lag, and routing parameter. However, there are limits to how much calibration can

improve runoff and streamflow process representations in the MCB because of the inadequate number of rainfall gages. Calibration using inadequate precipitation gages can result in unrealistic land surface parameter selection. There may also be inaccuracies in streamflow measurement during the study period due to heavy vegetation, ice jam, beaver dams, and human related obstructions (C. Laveau, personal communication, 2017).
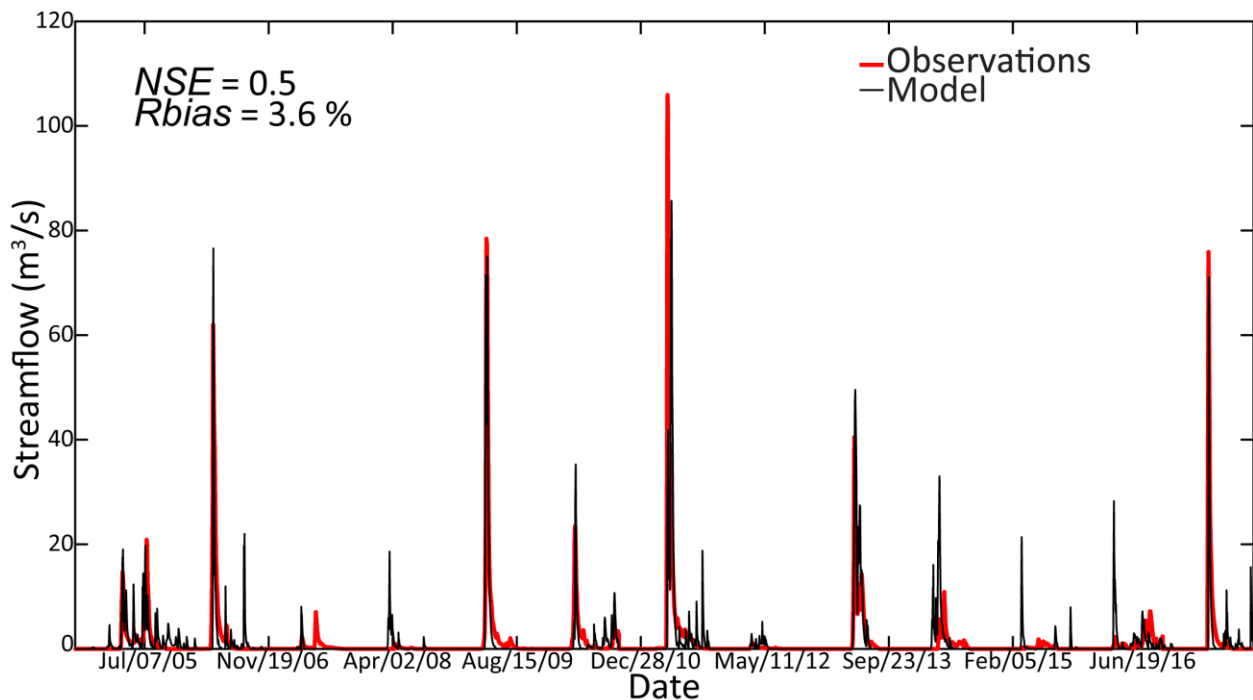

Figure 10. Streamflow Model Evaluation. The red line represents observed streamflow at the USGS gage and the black line represents modeled streamflow. Time starts at September 30, 2004 and ends at September 30, 2017. The overall *NSE* is 0.5 and the *RBIAS* shows an overestimate by 3.6%.

Water Balance

Please note that all results past this point that are not from a reference or related to temperature are from the model.

Figure 11 shows the water balance using rainfall and snowfall as the input flux and ET, sublimation, canopy sublimation, and snow drift as the output flux. The highest contribution of

38

output flux for every year is ET while rainfall is the foremost contributor to input flux. The snowfall contribution is less than 30.0% of total input flux but is highly variable from year to year. Overall, there were significant gains of subsurface storage during 2005-10 (the first half of the simulation period) while, both subsurface storage addition and depletion were detected during the post-2010 period (see the numbers above the bars in Figure 11 for storage change amounts). Note that the storage losses (given as negative numbers above the bars in Figure 11) were influenced by streamflow, ET, and snow related processes. Streamflow, ET, drift, and sublimation resulted in storage depletion during two wet years (2011 and 2017) while ET is the only flux causing storage depletion during a dry year (2012). In contrast, relatively dry years like 2007-08 still experienced a net increase in storage likely due to low ET and loss of snow due to drift and sublimation. The year 2009-10 despite having the highest precipitation was not able to yield the high streamflow but received maximum gains to subsurface storage via infiltration resulting in elevated fall soil moisture. Note that the precipitation was later in the summer of 2010, primarily in August (81.1 mm at Cando and 166.4 at Rolla) and September (144.6 mm at Rolla and 96.3 mm at Cando). High streamflow in the spring of 2011 is probably the main contributor along with high precipitation to the sharp rise in 2011 of the lake levels in Lake Irvine (Vandeberg et al., 2015). Another wet year 2013 was also a flood year with a higher amount of precipitation than ET leading to an increase in storage. The year 2013 experienced a tri-modal streamflow pattern, which did not fully recess between peaks. The first and largest peak being from a mixture of rain and snow, and the next two being from the rain with the second being slightly larger than the first. It is possible that the slight increase in storage post-2011 is partially caused by backwash from the rise of Lake Irvine, which in 2015 started to drop again (Vandeberg et al., 2015).
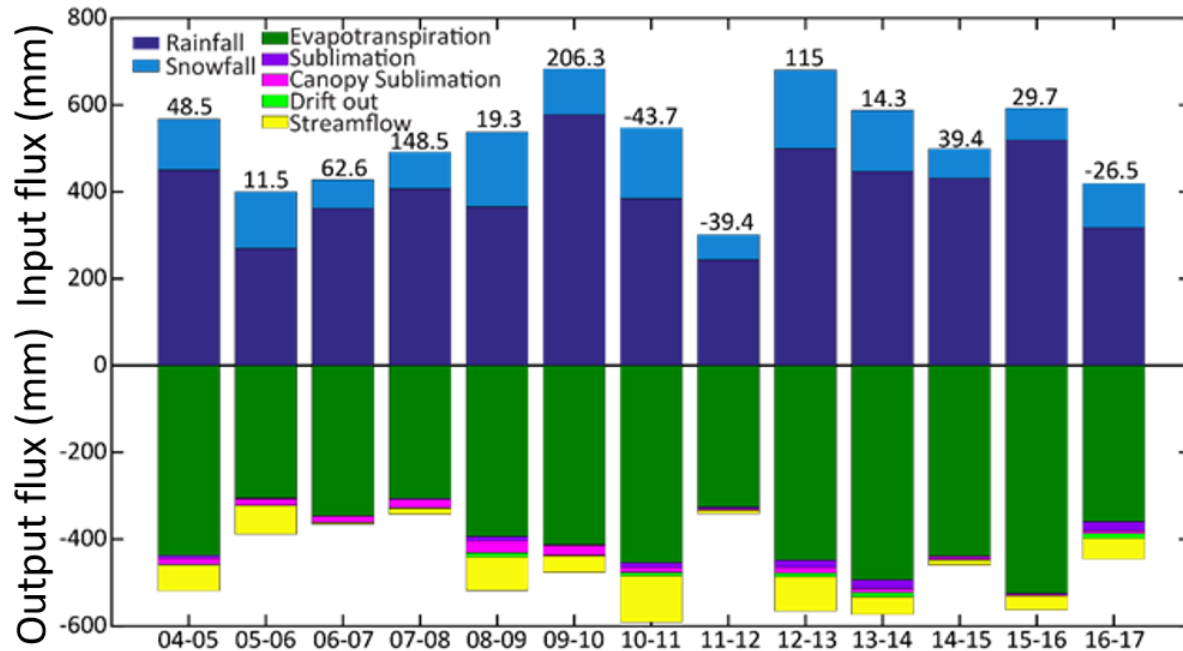
Figure 11. Water Balance from Model. Input flux is represented by precipitation with light blue as snow and dark blue as rain. Output flux is represented by sublimation (purple), canopy sublimation (pink), snow drift (bright green), ET (dark green), and streamflow (yellow). The numbers above each bar are the change in storage in mm.

Figure 11 clearly shows the dominance of ET in the MCB hydrologic cycle, which is expected since most of the basin is covered in some form of vegetation throughout the spring, summer, and early fall months. Summer ET in prairies in the NGP accounts for as much as 60.0% of the total ET (Hayashi et al., 1998; Nachshon et al., 2013). For Devils Lake the maximum ET occurs in July and August and that ET often exceeds precipitation from April to October (Hoerling et al., 2010). There is a direct relationship between annual rainfall and ET in all years of the study period (Figure 12; Table 4). This relationship was also noted by Mahmood et al. (2017) in a study of the southern Canadian Prairies. In contrast, there is no obvious correlation between ET and total yearly snowfall (Figure 12; Table 4). Total ET does not show a trend before 2008 ($R^2 \approx 0.46$). After 2008 there is a generally increasing trend with the exception of the dry years 2012, 2015, and 2017. This ET trend may also in part be related to increases in temperature as it was in modeling results for future climate changes scenarios that included

warming (Bonsal et al., 2017; Trenbeth, 2011; Collins et al., 2013; Rasouli et al., 2014). A water

budget based model in Devils Lake indicated that both potential and actual ET increased from

the period of 1907-1980 to the period from 1981 to 2011 when the study ended (Todhunter &
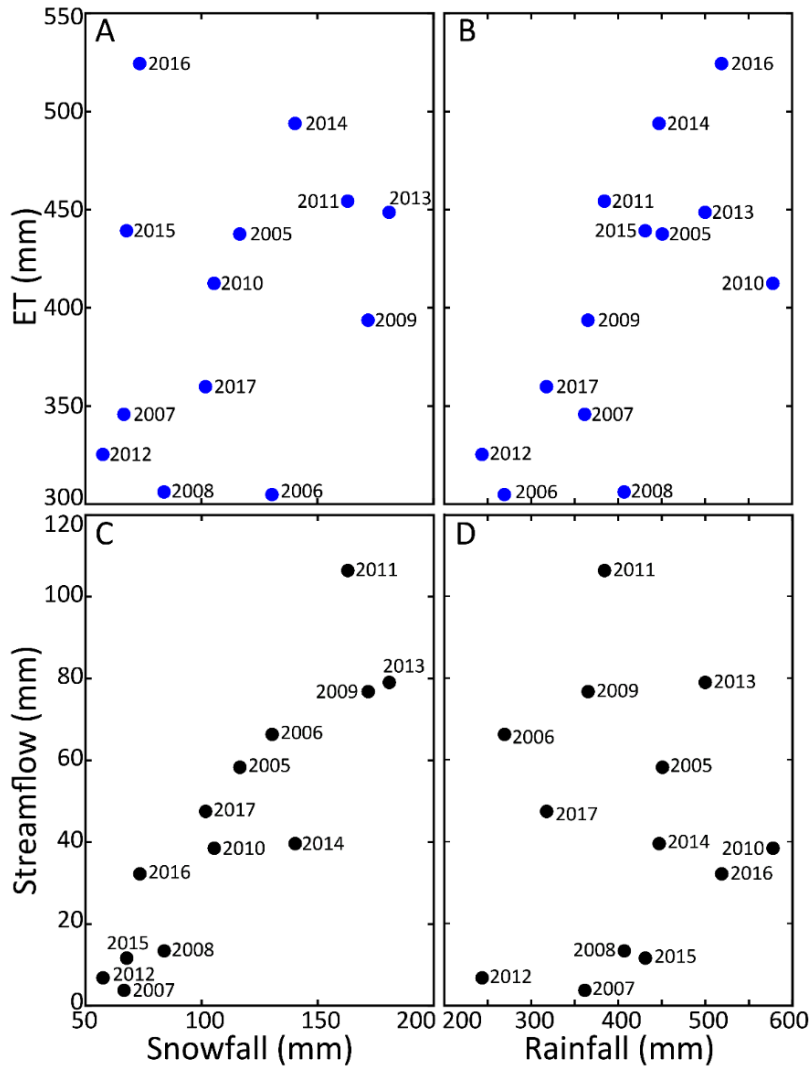
Fietzek-DeVries, 2016).

Figure 12. ET and Streamflow Comparison to Precipitation by Phase. A: ET vs. snowfall. B: ET vs. rainfall. C: Streamflow vs. snowfall. D: Streamflow vs. rainfall. Each dot represents a water year from September 30 to September 30 and is label with the year at the end of the period.

Table 4. Pearson Product Moment Correlation Coefficient (r) for ET vs. Rain, ET vs. Snow, Streamflow vs. Rain and Streamflow vs. Snow.

independent variable	dependent variable	Pearson r
Rain	ET	0.69
Snow	ET	0.27
Rain	Streamflow	0.06
Snow	Streamflow	0.90

In all years rain is the dominant form of precipitation. However it is not the dominant factor in determining streamflow. This can be witnessed in Figure 12 and Table 4 where snowfall and streamflow have a correlation while streamflow and rainfall have no apparent relationship. Over the period from 2004-17 there is no apparent trend in annual streamflow totals. However, the overall annual streamflow during and pre-2011 is higher than the post-2011 period. There were substantial amounts of streamflow during 2005, 2006, 2009, and 2011 year while the years having large streamflow in the post-2011 period were 2013 and 2017. Only two major rainfall-induced streamflow events were detected. One occurred in the summer of 2005 from approximately June 26 to August 2 and the other occurred in the summer of 2016 from approximately August 3 to September 4 (Figure 10). Spring rain also resulted in streamflow via both direct runoff generation and ROS in some years such as 2013.

Sublimation is a more significant contributor to the output flux of snow than drift, which is negligible in all but the wettest years i.e. 2008-09, 2010-11, 2013-14, and 2016-17. This is in agreement with a study done at Havikpak Creek, which is an Arctic basin, where sublimation from blowing snow combined with canopy sublimation and surface sublimation averaged 47.0 mm/yr, whereas blowing snow transport averaged 2.0 mm/yr. (Krogh et al., 2017). It also matches with the finding that in Canadian forest blowing snow transport was minimal (Pomeroy et al.,1999; Pomeroy et al., 2007). However, it contradicts the finding of Pomeroy & Gray (1995)

that for open fields sublimation was only slightly higher than blowing snow transport (Pomeroy et al., 2007).

Hydrological Changes

In addition to water balance, the relative contribution of vertical flux and the runoff ratio was further inspected. In Figure 13, the x-axis represents the vertical output flux fraction (ET + sublimation+ canopy sublimation)/ annual precipitation, while the y-axis represents the runoff ratio (Q/P). Overall, Figure 12 clearly displays that vertical flux plays a dominant role in partitioning precipitation during the simulation period. Note that the contribution of ET is more than 95.0% of total vertical flux. The dominance of vertical flux is extreme during the post-2011 period while both streamflow and vertical flux (ET) are governing fluxes influencing water budget in pre-2011 periods. The Q/P values in the pre-2011 period are highly variable and fluctuate between 0.01 and 0.2. In contrast for the post-2011 period, the range of Q/P variation is between 0.02 and 0.12. It is hypothesized that the MCB hydrologic cycle switched from a less ET controlled system with a relatively higher contribution from streamflow in pre-2011 to an extreme ET dominated system with low contribution from streamflow. The transition of the degree of ET dominance can be attributed to a shift in rainfall and daytime cloud cover period. In the pre-2011 period, average spring/summer rainfall (340.0 mm) is lower than the post-2011 period (355.0 mm) (Table 3). Monthly rainfall during May, June, July, and September are higher for the post-2011 period than the pre-2011 period. Note that during these months, the evaporative demand is high due to higher temperature and longer sunshine hours. However, August precipitation during the pre-2011 period is higher than in the post-2011 period. Most of crops are harvested during the month of August. Similarly, the cloud cover hours (relative humidity > 90.0%) play a role on the switch of the intensity of ET dominance. In the pre-2011 period,

overcast conditions lasted for 280.0 hours while the cloud cover hours during post-2011 were

228.0 hours. Cloud cover hours are significantly higher in pre-2011 during the months of June
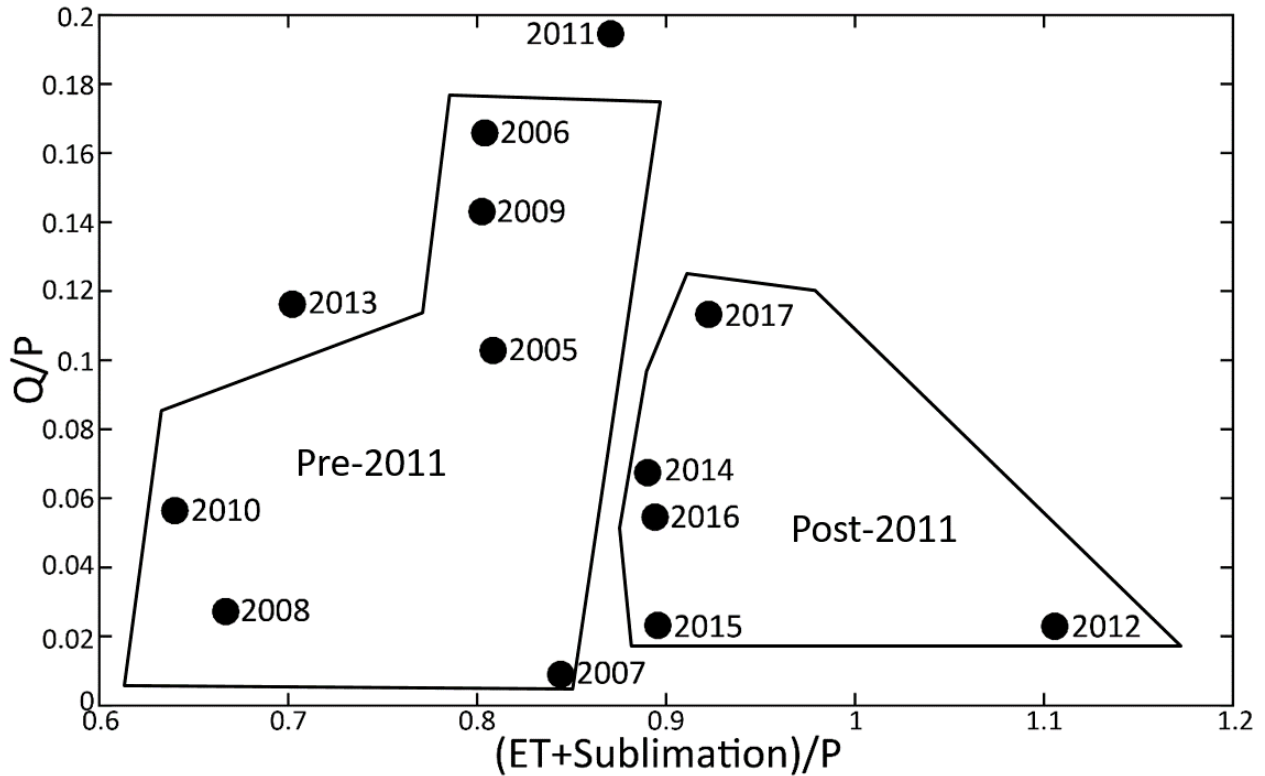
and August.

Figure 13. Runoff Ratio Versus Vertical flux. The runoff ratio is the total yearly streamflow divided by total yearly precipitation. Vertical flux is total yearly ET plus sublimation divided by total yearly precipitation. Each black dot represents a water year from September 30 to September 30 and is labeled with the year at the end of the period.

Dumanski et al. (2015) recently reported a hydrologic regime change via a dramatic

increase in peak streamflow, substantial discharge contribution from rainfall, and a transition

from unimodal to the bimodal hydrograph in the SCRB during the post-2011 period compared to

the period between 1975 and 2010. However, in Coles et al. (2016) there was substantial increase

in rainfall that had little no impact on runoff at a hillslope scale (Swift Current, SK). These

outcomes improve the current knowledge by reporting the elevated dominance of ET in the post-

2011 period. The results suggest a noticeable decline in streamflow during the post-2011 period

compared to the pre-2011 period. The lack of sensitivity of streamflow to increased rainfall is partly due to low rainfall rates (Mahmood et al., 2017) and high evaporative demand during the spring and summer period. To produce basin-wide streamflow, a few consecutive heavy rainfall days are needed (Mahmood et al., 2017) which was only observed in the 2005 summer period. The climate models used in various studies (e.g. Masud et al., 2016; Mladjic et al., 2011) project an overall increased in rainfall in the NGP watersheds. Our findings suggest that the rainfall is increasing during the current wet period and the MCB responds to such elevated rainfall by evapotranspiring more water from the system.

Temperature has been noticeably changing in the study area. The data collected from NDAWN for Cando, ND from 2002 to 2017 shows a trend in the increase in temperature for every month except April, November, and December based on average monthly temperatures (Table 5). This observation is an agreement with a study of (SCRB), where from 1940 to 2014 monthly temperature has increased anywhere from 1.1 to 4.0°C (Dumanski et al., 2015). It also aligns with findings from a study of trends from 1980 to 2013 in North Dakota from July to October, which exhibited an increase in minimum temperature of ≥0.31 °C per decade, a ≥0.31 °C per decade increase in the maximum temperature in September, and a decrease in average temperature from April to June (Dai et al., 2016). More locally it agrees with a study for Devils Lake, which concluded that the temperature has increased between the period of 1907-1980 to 1981 to 2011 with a larger change in the months of November to March than from May through September (Todhunter & Fietzek-DeVries, 2016). Over the period from 2004-17 there has been an increasing trend in rain and a decreasing trend in snow. This finding is agreement with the study of Dumanski et al. (2015) in Canadian Prairies that had an increase in yearly rainfall of 0.9 mm per year with a decrease in snowfall of 0.5 mm per year from 1942 to 2014 (2015). It also

agrees with findings for spring to summer precipitation trends for 1980 to 2013 in North Dakota, which had a median increase in precipitation from April to June of about 25.0 mm per decade (Dai et al., 2016). It is disagreement with the finding that precipitation in cold months (November to March) increased at Devils Lake from the period 1907-1980 to the period 1981-2011 by 6.7 mm (Todhunter & Fietzek-DeVries, 2016) although some of that was possibly rain. This study also found that for the same period warm season precipitation (May to September) increased by 63.1 mm (Todhunter & Fietzek-DeVries (2016). Decreases in snowfall can have a very adverse impact on farmers that are dependent of snowmelt based water for crop irrigation in the spring. These changes in precipitation amount are in part related to changes in atmospheric circulation patterns and changes in temperature (Bonsal et al., 2017; Kluver & Leathers, 2015). Snow data from 1930 to 2006 illustrates that in northeastern North Dakota, the Pacific/North American Pattern (PNA), the Pacific Decadal Oscillation, and the Northern Hemisphere temperature had the strongest influence on the frequency of snowfall events of greater than or equal to 50.8 mm (Kluver & Leathers, 2015). In that study the North Atlantic Oscillation and PNA had the strongest influence on the total winter snowfall amount (Kluver & Leathers, 2015). PNA is related to the East Asian Jetstream that when positive results in below average precipitation in the Upper Midwest (Climate Prediction Center Internet Team, 2012). January's El Niño Southern Oscillation is negatively related to snow, since it results in a warm winter (Kluver & Leathers, 2015; Climate Prediction Center Internet Team, 2017). The DLB is thought to currently be in a period on increased El Niño activity, which can help account for warmer winters similar to 2017 (Wiche et al., 2000). On a more local scale a mid-tropospheric ridge over the prairies blocks incoming precipitation from the Pacific Ocean and the Gulf of Mexico leading to drier conditions (Bonsal et al., 2017; Chakaravarti, 1976; Dey, 1982; Liu et al., 2004). Not

only is the amount of rain and snow changing between years, but the proportion of rain to snow in a year is also changing. Over the study period of water year 2004-17 there has been a slight increase in the fraction of rain to total precipitation with a corresponding slight decrease in the fraction of snow to the total. Dumanski et al. (2015) had a similar finding with a 10.0% increase in the rainfall fraction from 1942 to 2014.

Table 5. Mann-Kendall Trend Analysis of Monthly Average Temperature for Cando, ND from 2002-17.

Monthly Average Temperature	Z-score	Confidence Interval
January	0.59	70.0
February	0.23	50.0
March	0.77	70.0
April	-0.68	75.0
May	1.76	95.0
June	0.77	75.0
July	0.50	65.0
August	1.40	90.0
September	1.22	85.0
October	1.13	85.0
November	-0.05	50.0
December	-0.50	65.0

These changes in climate can perhaps best be noticed through changes in streamflow and extreme streamflow events. 2005 had a rain related streamflow peak in the summer in both the gage and the model (Figure 10). That year, the Canadian provinces of Alberta, Saskatchewan, and Manitoba experienced heavy flooding linked to a rain storm from 1-4 June (Shook, 2016). The 2011 flood mentioned above was also documented in the SCRB where it was related to a

mix of snowmelt and rainfall runoff (Dumanski et al., 2015). This event is thought to be a turning point to a much higher fraction of mixed runoff to total runoff (6% from 1995-2010 and 19% from 2010-14 at the SCRB) (Dumanski et al., 2015). Mixed runoff is runoff that is created by combining rainfall runoff with snowmelt. As the weather warms and rain becomes more prevalent there has been a change from the normal unimodal snowmelt induced streamflow to a more multimodal streamflow. This can be perceived in the gage data for 2005, 2013, 2014, 2015, and 2016 (Figure 10). In the case of 2005 and post-2013 these peaks are larger than the snowmelt peak (Figure 10). In the SCRB there were similar peaks in 2012 and 2014 with 2012 being the first on record (Dumanski et al., 2015). In 2014 peaks also occurred in the Assiniboine, Souris, and Qu' Appelle River Basin where there was summer flooding due to above average rainfall from April to June, high soil moisture, and at capacity depressions (Ahmari et al., 2016). This widespread flooding is absent in the study area.

Mechanisms of Hydrological Change

Rain-On-Snow

ROS can be a significant contributor to floods. Rain adds advective energy to the snowpack helping to increase melt rates (Pomeroy et al., 2016). During rainfall, the air is saturated to some extent, which allows for latent heat transfer to the snowpack (Pomeroy et al., 2016). The fact that the air temperature is above the freezing point of water adds sensible heat to the snowpack (Pomeroy et al., 2016). The rain combines with the melting snow to create a higher quantity of runoff than snowmelt alone over frozen or partially frozen soil, which allows for limited infiltration (Mahmood et al., 2017). The ROS contribution during the study period is an available output from the CRHM model. ROS was a key contributor to streamflow in 2005 and

2010, and a noticeable contributor in 2009, 2011, and 2013 (Figure 14). 2005 was snow-covered

until the beginning of April when the snow started to melt slowly, providing an opportunity for

the occurrence of ROS (Figure 15). 2009 was similar to 2005 but had a snowpack that melted

rapidly, reducing the amount of time where ROS was possible (Figure 15). 2010 had the largest

contribution of ROS for the study period, which resulted in a relatively rapid snowmelt (Figures

14 & 15). In 2011 the snow melted faster than 2005 but slower than 2009. Due to a below

freezing average temperature in March and an April with an average temperature of ~3.0°C in

2011 the snow started melting later than previous years (Figure 15). The year 2011 also had the

third largest snowfall providing time for ROS to occur prior to complete snowmelt (Table 1).

2013 saw the coldest average temperatures for March and April with -11.6°C and -3.5°C

respectively. This allowed the snowpack to persist longer than in other years, and ROS to occur

primarily in the middle of May. ROS in June of 2013 was cited as one of the causes of the 2013

flood in the Canadian Rockies, showing that ROS in 2013 was a widespread phenomenon

affecting both prairie and mountainous regions (Pomeroy et al., 2016). If the temperature in

Northern Great Plains continues to warm in March and fluctuate in April, ROS could become an

increasingly more common event in a region where it only recently has started to occur

(Pomeroy et al., 2016; Dumanski et al., 2015; Stadnyk et al., 2016). The results of this study

show that the post-2011 period had a smaller ROS contribution than the pre-2011 period.

Excluding the very dry year of 2012 the period after 2011 has higher rainfall by ~37.6 mm. This

shows that the rainfall timing is clearly more important than the rainfall amount for ROS

processes. The temporal extent and thickness of snowpack are also important factors in

determining the amount of time when ROS is possible, and thus the amount of ROS.
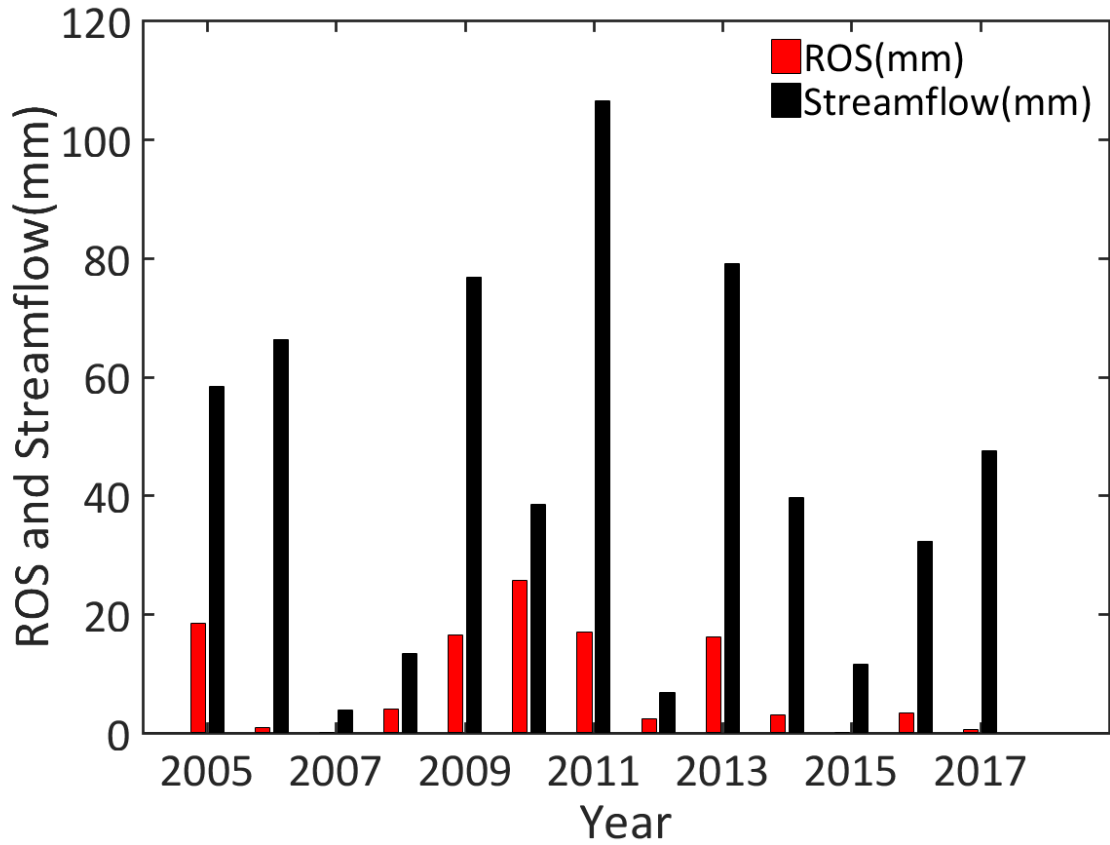

Figure 14. ROS and Streamflow by Water Year. Red bars represent ROS from CRHM model output. Black bars represent streamflow also from the model.
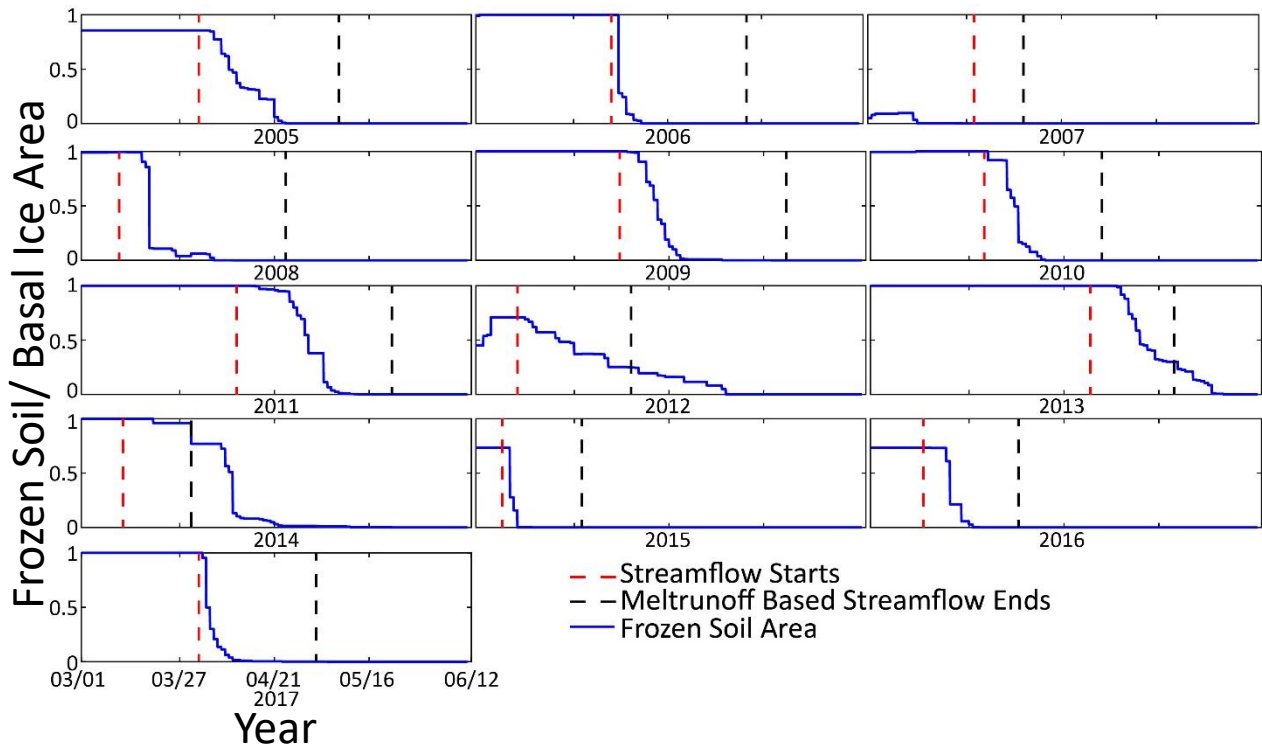
Figure 15. Frozen Soil/ Basal Ice Area and Timing of Melt Runoff Related Streamflow. The blue line represents the fractional area of the basin that is frozen versus time from model output based on equation 1. The red dashed line is the approximate beginning of streamflow and the black dashed line is the end of the first peak of the hydrograph. The red and black dashed lines are based on model output.

Soil Moisture and Frozen Soil Conditions

Soil moisture conditions in the fall can have an impact on spring streamflow. Water that infiltrates in fall and that does not go to ET can create a frozen layer in the soil due to below freezing temperatures near the surface in winter. If the fall is wetter than average as it was in 2008, 2010, 2017 a deep ice layer can form. There were also ice layers in a modeling study for South Tobacco Creek in years having a wet winter i.e. 2004-05, 2008-09, and 2010-11 (Mahmood et al., 2017). If the following spring has a long period of below freezing or near freezing temperatures, then the frozen layer persists well into spring contributing to increased melt runoff related flooding. This was the case in 2009 and 2011 when March had an average temperature of ~-8.0°C and April had an average temperature ~3.0°C. Snowpack conditions

including thickness, area, and temporal extent can also have an impact on the duration of frozen soil conditions, since the pack acts as an insulating layer. These were also given as factors that impact the ability of water to infiltrate frozen soil at a hillslope scale (Coles et al., 2016). Often due to midseason melt and refreeze a layer of ice will form at the soil surface or subsurface (Mahmood et al., 2017; Coles et al., 2016). This was seen at many sites during the 2017 snow survey due to a warm February and March. As the temperature continues to increase in January, February, and March these ice layers often referred to as basal ice could become more common. It is also thought that they can occur due to ROS events, which could become more prevalent with an increase in March rainfall (Dumanski et al., 2015; Mahmood et al., 2017). This happens because the rain percolates through the snowpack and the water, being unable to infiltrate, freezes as a surface ice layer due to below freezing night-time temperatures (Dumanski et al., 2015). When the soil and surface ice thaw in the spring the water can infiltrate further into the ground, raise the groundwater table, and become a source of water for vegetation adding to summer ET totals.

Soil moisture and streamflow were highly variable pre-2011 (Figure 16). Streamflow with the exception of 2006 is well correlated with soil moisture. It is possible that 2006 incorrectly shows low soil moisture and high streamflow since the model overestimated rainfall only related streamflow in 2006. Post-2011 soil moisture on average was higher than pre-2011 (Figure 16) but, with the exception of 2013, streamflow was lower than the high streamflow years pre-2011 (i.e., 2005,2006,2009). For the dry period of 2006-08 low antecedent soil moisture matches well with the low streamflow likely because the snow meltwater has the ability to infiltrate the soil and goes toward ET later in the year (Fang & Pomeroy, 2007; Granger et al., 1984; Gray et al., 1986; Mahmood et al., 2017). For the flood years of 2009 and 2011 there is a

strong relationship between antecedent soil moisture conditions and streamflow because of reduced infiltration capacity and the presence of frozen soil, which was also the case for these years in South Tobacco Creek (Mahmood et al., 2017). This is not seen in the flood year of 2013 because 2012 was a dry year. In an assessment of the Assiniboine flood of 2014 it was stated that the soil moisture conditions have been "extremely wet" since prior to 2011 (Ahmari et al., 2016). This agrees with the results for the study area where soil moisture has been moderate to above average since 2009.

Figure 15 shows the frozen soil and/or basal ice layer status in the MCB during spring streamflow period for each simulation year. The y-axis represents a ratio of frozen soil and/or basal ice area to total MCB area. Some years have a common pattern in the shape of the thaw curve (Figure 15). 2006 and 2017 both had a sharp drop followed by a short curve. The curve was caused by the depressions melting later than other areas. The sharp drop was likely due to an abrupt rise in temperatures. 2009 and 2011 had an almost linear decrease and had an average temperature during the rising limb of streamflow of 4.5 and 4.3°C, respectively. These two years also were only separated by 0.5 mm of ROS. There was also a match between the year 2015 and 2016, which were similar to 2006 and 2017 but due to a smaller snowpack did not freeze completely. There is some difference seen in the thaw rate pre-2011 compared to post-2011. The average based on the time it takes to go from the maximum frozen soil area to completely unfrozen conditions for pre-2011 and post-2011 are ~61.0 km^2/day and ~41.4 km^2/day. Thaw rate is mostly controlled by the size of the snowpack, temperature and soil moisture conditions all of which can be highly variable in the study area from year to year.

The following is a closer examination of frozen soil and surface conditions on a yearly basis starting with the pre-2011 period. In 2005 soil was frozen until early April and thawed

slowly likely due to the fact that the average temperature in March was -4.7°C. 2006 had an April with an average temperature of ~8.6°C and relatively low soil moisture, which made for a rapid thawing of the soil (Figures 14 & 15). The years 2005 and 2009 were on average 72.0% and 83.0% respectively, frozen during the rising limb of streamflow. This increased the size of the melt related runoff peak. In comparison 2006 had an average on 52.0% of the basin frozen during the rising limb of streamflow. 2006 also had low soil moisture due to a relatively dry fall in 2005 (Figure 16). Unlike 2005, which had a large rainfall related streamflow peak, streamflow in 2006 only had one melt-related peak in the gage data. However, 2006 had higher streamflow than 2005. This is in part due to the slightly larger snowpack. Also examining ROS based on the occurrence of rain during periods of snowcover instead of using model output it was determined that 2006 had a noticeable contribution from ROS that added to streamflow and could be the reason for the rapid melting of snow and soil. 2007 having low antecedent soil moisture and low snow accumulation, only saw frozen soil in a small fraction of the basin, and was completely unfrozen during streamflow (Figures 14 & 15). This is consistent with the finding by Mahmood et al. (2017) that there was an absence of ice lenses in years with a dry winter. The year 2008 also had low antecedent soil moisture conditions and low snow accumulation (Figures 10 & 15). March of 2008 saw below freezing temperatures with snowstorms late into the month causing the short periods of increased frozen soil after the initial rapid decline (Figure 15). 2006-07 had almost no snowfall until March, which was too little too late to freeze the soil. In comparison the dry water year of 2007-08 had higher snowfall in December that densified and added to the later season snowfall in March allowing a portion of the basin to be frozen during the rising limb of streamflow. 2009 had a relatively steady rate of thaw in mid-April (Figure 15). This make sense in light of the fact that the average temperature in March was -8.1°C, there was the highest

snowfall in 2009 of any year, and a moderate contribution from ROS in mid to Late-April

(Figures 11 & 14). 2010 did not start thawing until early April, but then thawed quickly due to

ROS and the second highest average temperature in April (Figure 15).

To continue the discussion of frozen soil here is a description of water year 2011. As

mentioned above 2010 saw a high amount of rainfall in August and September. This led to high

soil moisture for the fall of 2010 that, along with below freezing winter temperatures (averaging

~ -13.0°C from December 2010-March 2011 at Cando, ND) caused a deeper and larger than

normal layer of frozen soil in the MCB and the Red River of the North Basin on the Canadian

side, and was given as a factor in the Canadian flood of 2011 (Stadnyk et al., 2016). The frozen

soil layer in the study area thawed slowly (Figure 15) throughout April and early May despite the

fact that the April and May temperatures in 2011 were about average and above freezing because

of the large snowpack in 2011 and the abnormal thickness of the frozen layer.

This discussion of frozen conditions will conclude with a look at the post-2011 period.

2012 had the slowest thaw rate of any of the years (Figure 15). This is partially due to the long

snowcover period in sub-basins one and two, which are at a slightly higher elevation than the rest

of the basin. It could also be related to the fact that while dry with minimal streamflow, 2012 had

moderate soil moisture because 2011 was a relatively wet year in comparison (Figure 16). The

year 2013 saw a later thaw than most years with an exponentially decreasing rate of thaw (Figure

15). Below freezing temperatures in the early morning occurred until May 12 and above freezing

temperatures were sporadic until late April, which can account for the late timing of thaw. The

decrease in the thaw rate can be attributed to low elevations with little vegetation thawing

quickly while higher and forested areas thawed slowly. 2014 saw a March that still averaged

below freezing, but a much warmer April than 2013 with only brief periods of below freezing

temperatures. The year 2014 had high snowfall that was spread throughout the season not allowing for much densification. This causes a low snow water equivalent that could account for the low streamflow despite the presence of frozen soil and the high antecedent soil moisture. March in both 2015 and 2016 were at least six degrees warmer on average than 2014, which combined with a small snowpack caused an earlier fast snowmelt (Figure 15). 2017 thawed quickly at the end of March; this is seen in both the model and in Mauvais Coulee streamflow data where the gage started recording on March 31 (Figure 15). This quick thaw is likely attributable to a sharp rise in temperature to above freezing on March 25. 2016 had fall rainfall runoff that led to 2017 having lower antecedent soil moisture than the previous year. The year 2017 had most of its snowfall at the beginning of the season allowing for densification that along with high snowfall increased the SWE. This allowed 2017 to have more streamflow than 2014 despite having lower snowfall and drier soil conditions. It was also observed in the field in 2017 that just prior to streamflow basal ice was common throughout the basin.
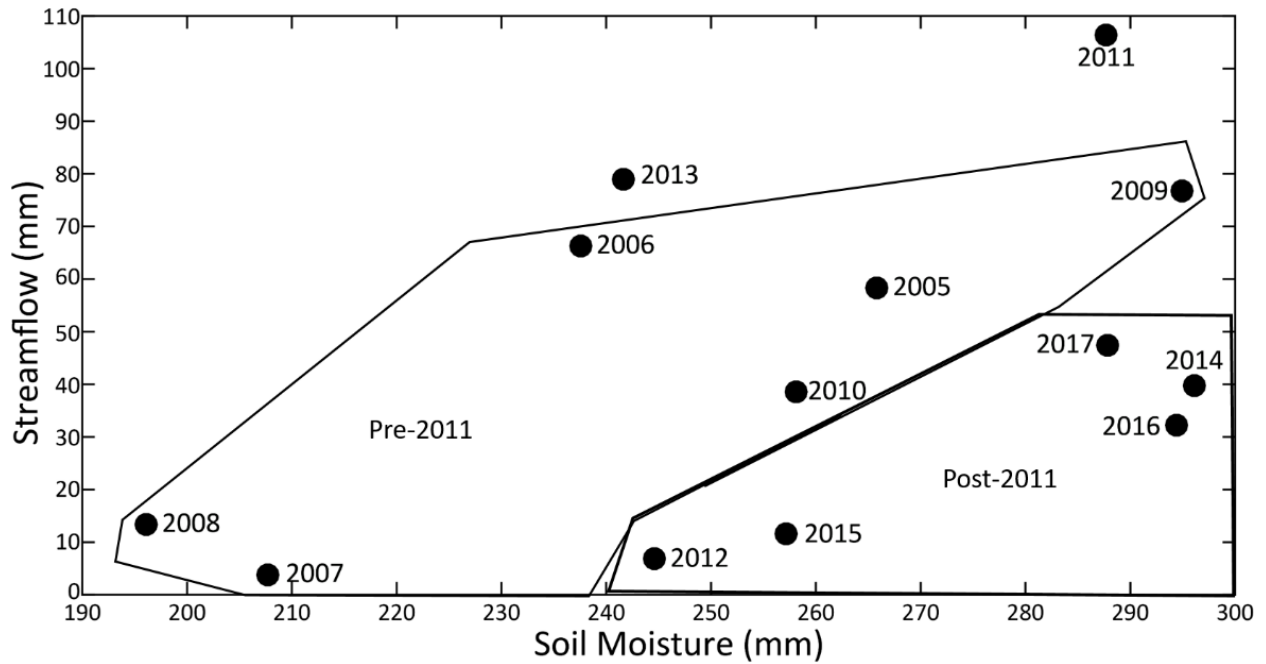
Figure 16. Streamflow Versus Antecedent Soil Moisture. Antecedent soil moisture is the moisture on November 1 of the water year which runs from September 30 to September 30. Dots are label based on the year that is at the end of the water year.

CHAPTER V

CONCLUSION

The NGP has experienced the impacts of the recent climate change over the last three decades through increases in precipitation and temperature. These changes can be attributed to global and regional atmospheric and oceanic circulation patterns (Kluver & Leathers, 2015; Wiche et al., 2000; Bonsal et al., 2017; Chakaravarti, 1976; Dey, 1982; Liu et al., 2004; Bonsal et al., 2017; Shabbar et al., 2011; Dey, 1977). A modular physically-based model was created using the Cold Region Hydrological Modeling platform to examine the impacts of these recent climate changes on hydrological processes. Over the modeling period of 2004-17 there has been an increase of the contribution of rain with a complementary decrease in the contribution of snow to overall precipitation. Impacts of this shift can be seen in the streamflow hydrographs with the presence of rainfall peaks in the years 2005, 2013, 2014, 2015, and 2016. The increase in rainfall also supplies more water for ET, which has been generally increasing since 2008. Differences in ET may also be related to increase in temperature and cloud cover in May through September when crops are growing and ET is at its highest. Since the year 2011, an increase in ET has made the water balance increasingly vertically flux dominated. Changes in snowfall and subsequent changes in snow accumulation have a direct relationship to the amount of sublimation, snow redistribution, snowmelt induced runoff, and streamflow. Through examination of modeling results and the snow survey, it was found that the highest, longest lasting accumulations tend to be in the higher elevation areas particularly, in the northwest

corner of the basin. Areas with higher vegetation height or density also have higher than average accumulation. Areas with higher accumulation are more robust in terms of being able to persist through mid-season warming periods. ROS events had a significant impact on streamflow in 2005, 2009, 2010, 2011, and the flood year of 2013 and have less of an impact after 2011 than they did before. Frozen soil is a key factor in limiting infiltration during the spring snowmelt period, which increases runoff as it did at the hill slope scale in Coles et al. (2016) and a smaller basin scale Mahmood et al. (2017). Spring frozen soil is strongly related to fall soil moisture conditions and was a contributor to the floods of 2009 and 2011, which were preceded by wet falls in 2008, and 2010 in the study area and Canada (Coles et al., 2016; Blais et al., 2016; Stadnyk et al., 2016). Dry years, such as 2007 and 2008 also show a relation between streamflow and antecedent soil moisture. These dry years are often poorly simulated by the CRHM model as they were for the La Salle Basin (Cordeiro et al., 2017). Streamflow is on average lower during the post-2011 period than during the pre-2011 period. This is in disagreement with the Dumanski et al. (2015) study, where there was significantly higher runoff for the period from 2011 to 2014 then there was prior to 2011. However, this difference may in part be related to the fact that in Dumanski et al. (2015) the study area had experienced a recent increase in agricultural drainage and wetland drainage, which was not experienced in the MCB. Overall, even in a time classified as a wet period there can still be substantial variability in hydrological processes, temperature, and precipitation between years. Below are some of the key observations that can be gleaned from the model results and the snow survey:

- Two phases exhibiting distinctive cold region hydrologic responses: pre and post-2011 period. During pre-2011 period, the MCB system was controlled by both streamflow and evapotranspiration (ET) while extreme ET dominance was

detected with very minor influence from streamflow in post-2011 period. The changes in the spring/summer rainfall and daytime overcast have led to an increase in ET in post-2011 period. The increase in ET caused a shift after 2011 to a more vertically flux dominated system.

- Sublimation is more important than drift in the erosion of snow and the overall water budget.

- Snow accumulation is highest at higher elevations and in areas of depressions or high vegetation. It along with the temperature and precipitation in March and April are key factors for the contribution of ROS to streamflow, which is lower after 2011 than it was before.

- Frozen soil related to antecedent soil moisture conditions is an important factor in increasing runoff, resulting in flooding in wet years like 2009 and 2011. In dry years like 2007 and 2012 frozen soil is spatially less extensive and plays little to no role in runoff.

Possible Improvements

All models can be improved with additional data and refinements. A field survey to examine stream conditions and locate culverts could improve the routing parameters and the position of the southern border of the watershed. The raster to polygon conversion in ArcMap is not perfect and could be improved upon by going through and reshaping polygons to aerial imagery. A module can be added in CRHM to simulate plant growth. This was not done for this study due to the amount of crop-related data that is needed on a seasonal basis. A module can also be added that was specifically designed for wetlands. However, wetlands only represent

~7.1% and are often disconnected from streamflow, thus adding this module would likely only lead to minimal improvement. In dry years of frozen soil, such as 2006 and 2008, the model could be improved by simulating cracks in the soil to allow limited infiltration (e.g. Cordeiro et al., 2017). Finally, the size and shape of wetlands and crops is not static thorough time. Wetlands often grow at the expense of croplands. Therefore, to create a more accurate model, these polygons and their size parameter in the model could be changed on a yearly basis.

Implications and Future Work

This model, possibly with some of these improvements, could be used for a variety of projects in the future. It could be used to forecast responses to future climate change or land use change scenarios. The model can also be expanded to include the rest of the Devils Lake Basin to help in the creation of flood hazard maps to help developers, farmers, and city planners. It could also be run further back it time to look at the cold region process in this area at a decadal scale to examine long term trends. It can also be used along with a dispersion model to examine spatiotemporal contamination patterns that impact water quality. In an agricultural basin such as Devils Lake contamination, from fertilizer and animal waste is quite common from phosphates and can led to harmful eutrophication in water ways. This has been experienced at Lake Winnipeg were above average flows have become more common (McCullough et al., 2012; Mahmood et al., 2017). As demand for food increases with increasing population areas of the DLB that are currently set aside for wetland conservation could be converted to agricultural land. This land cover conversion would exacerbate the pollution problem and could change snow accumulation and runoff flow amounts and spatial patterns.
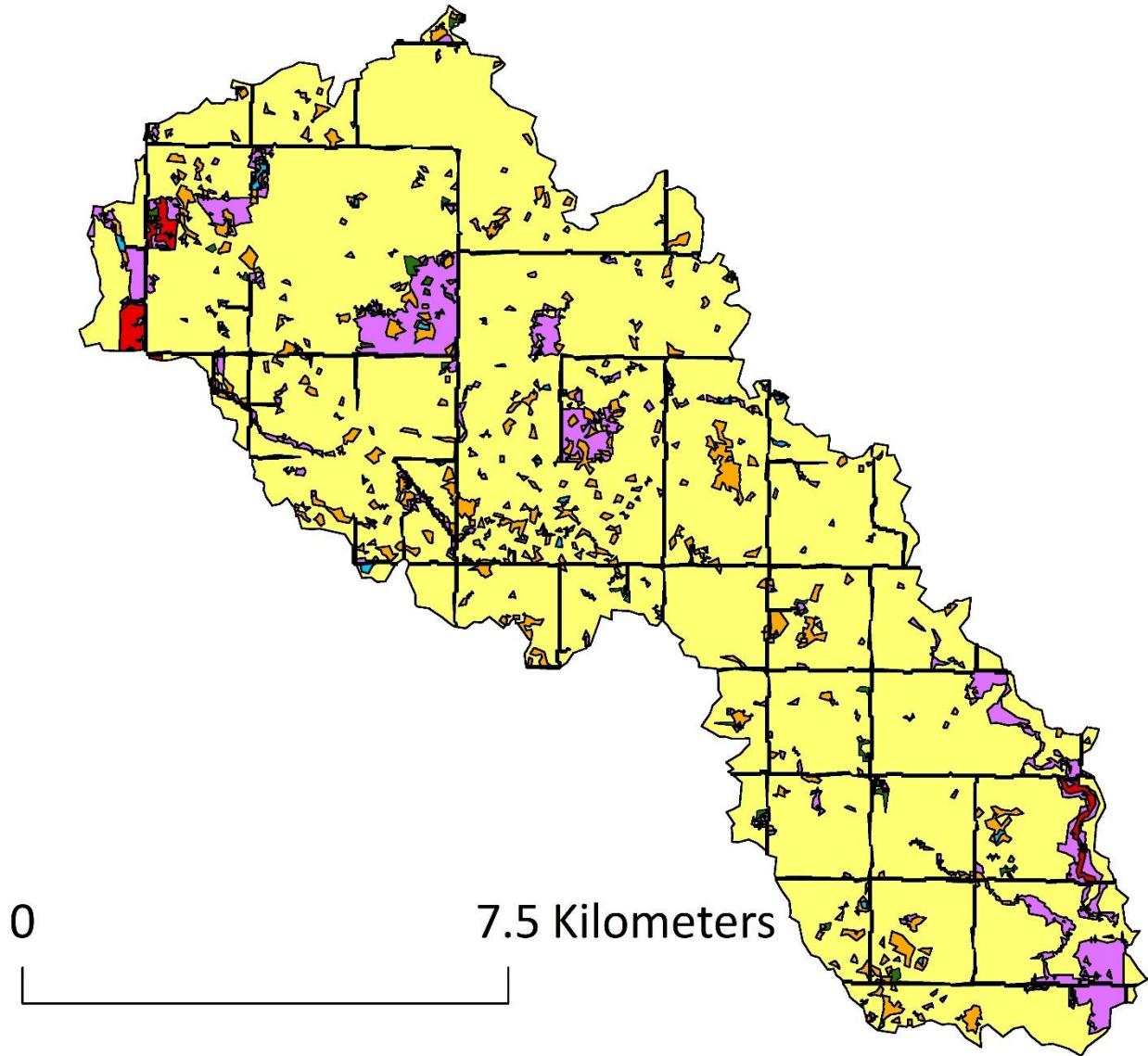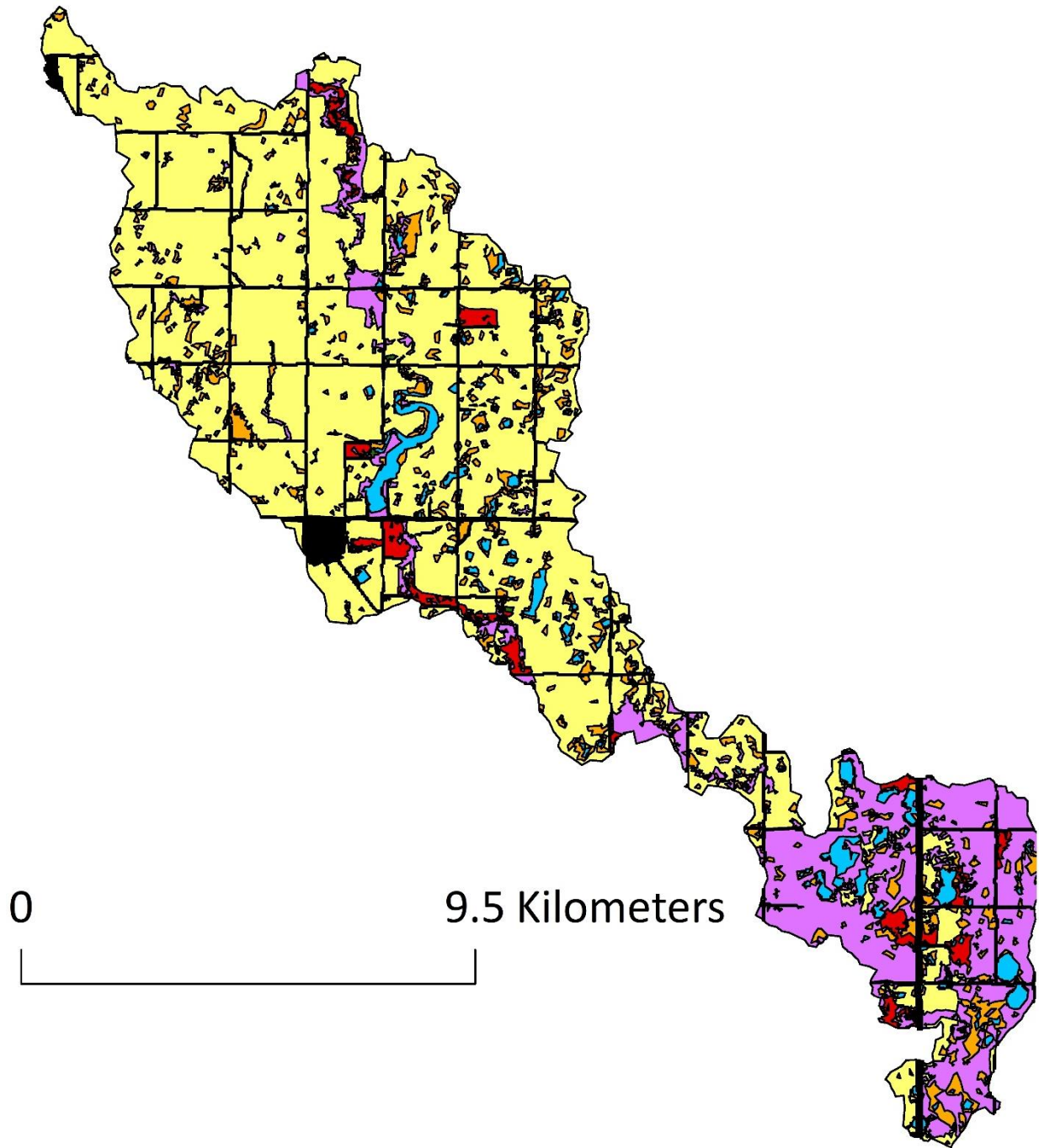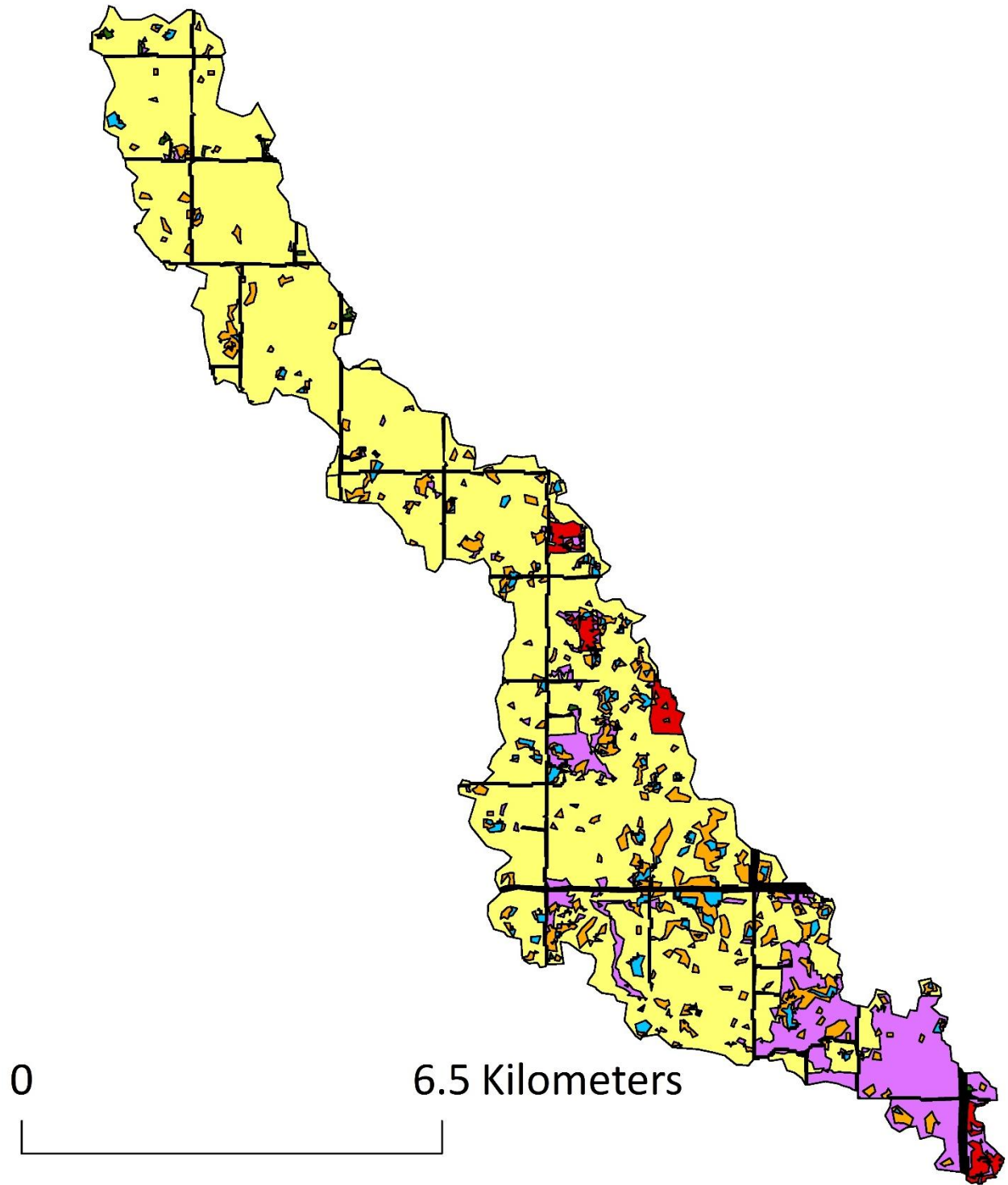
APPENDICES

Hydrological Response Units by Sub-Basin

Sub-basin 1

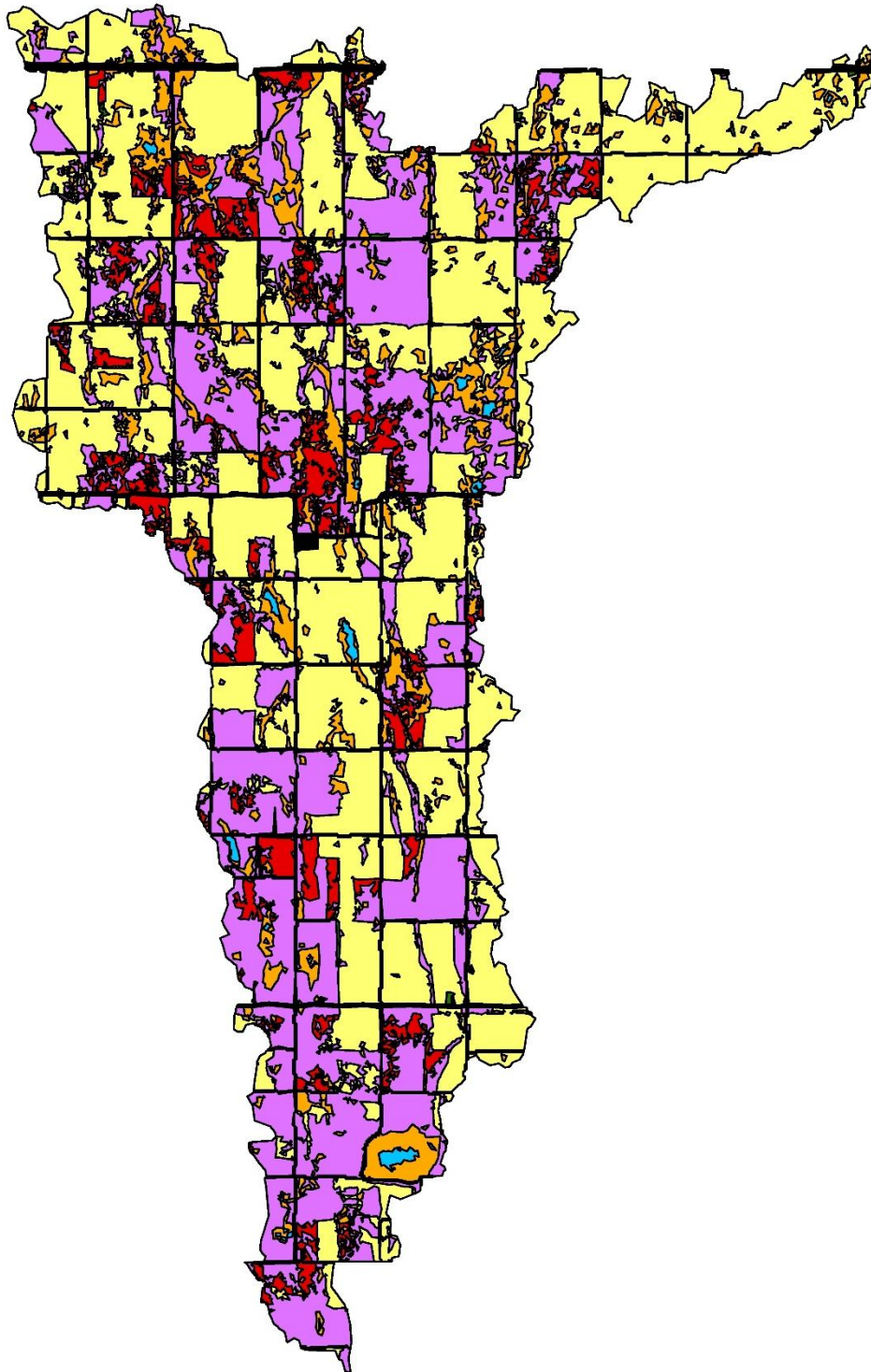0   7.5 Kilometers

Sub-basin 2

0　　　　　　　　　　　　9.5 Kilometers
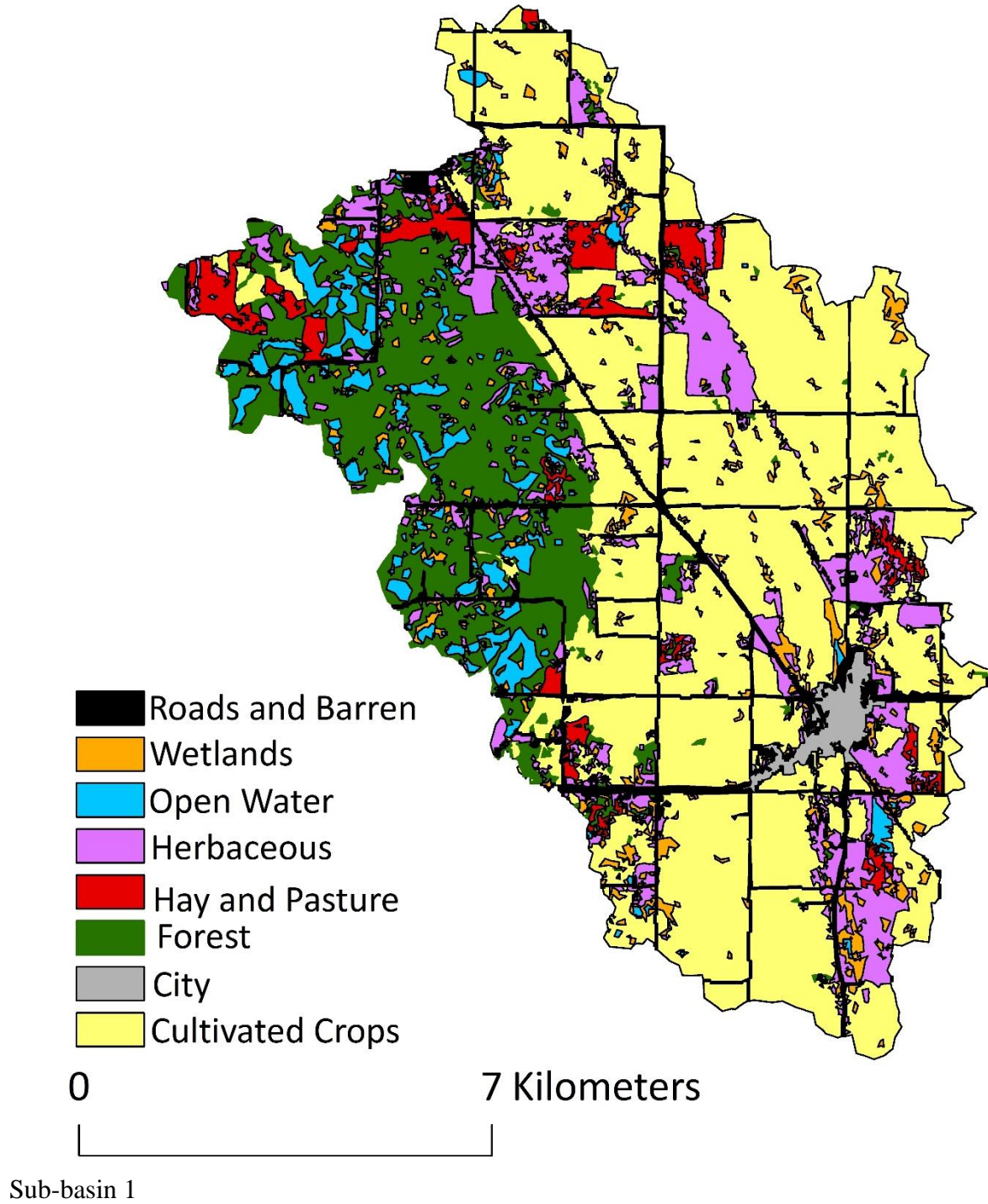
Sub-basin 3

0   6.5 Kilometers

Sub-basin 4
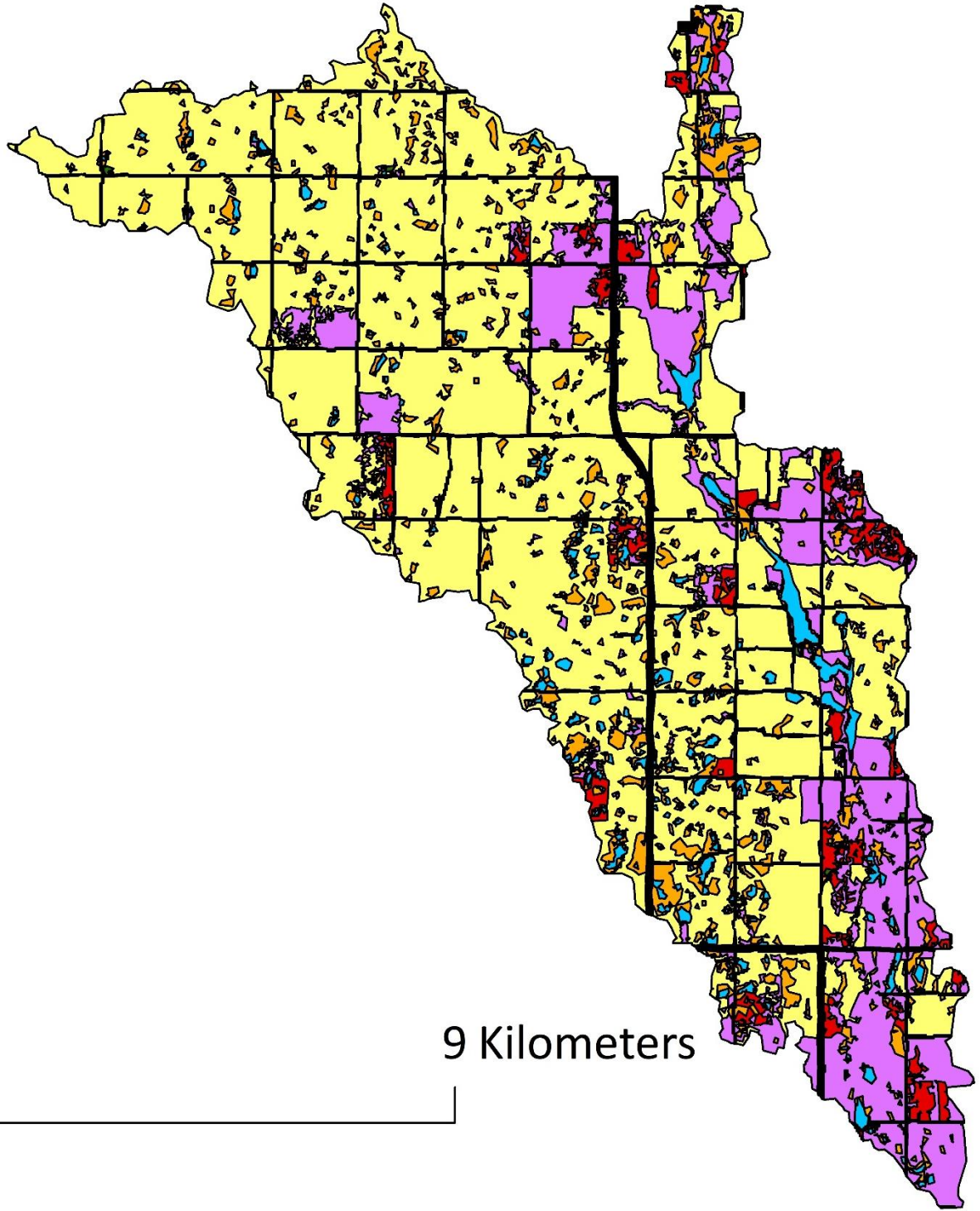
0　　　　　　　　　　　　　9 Kilometers
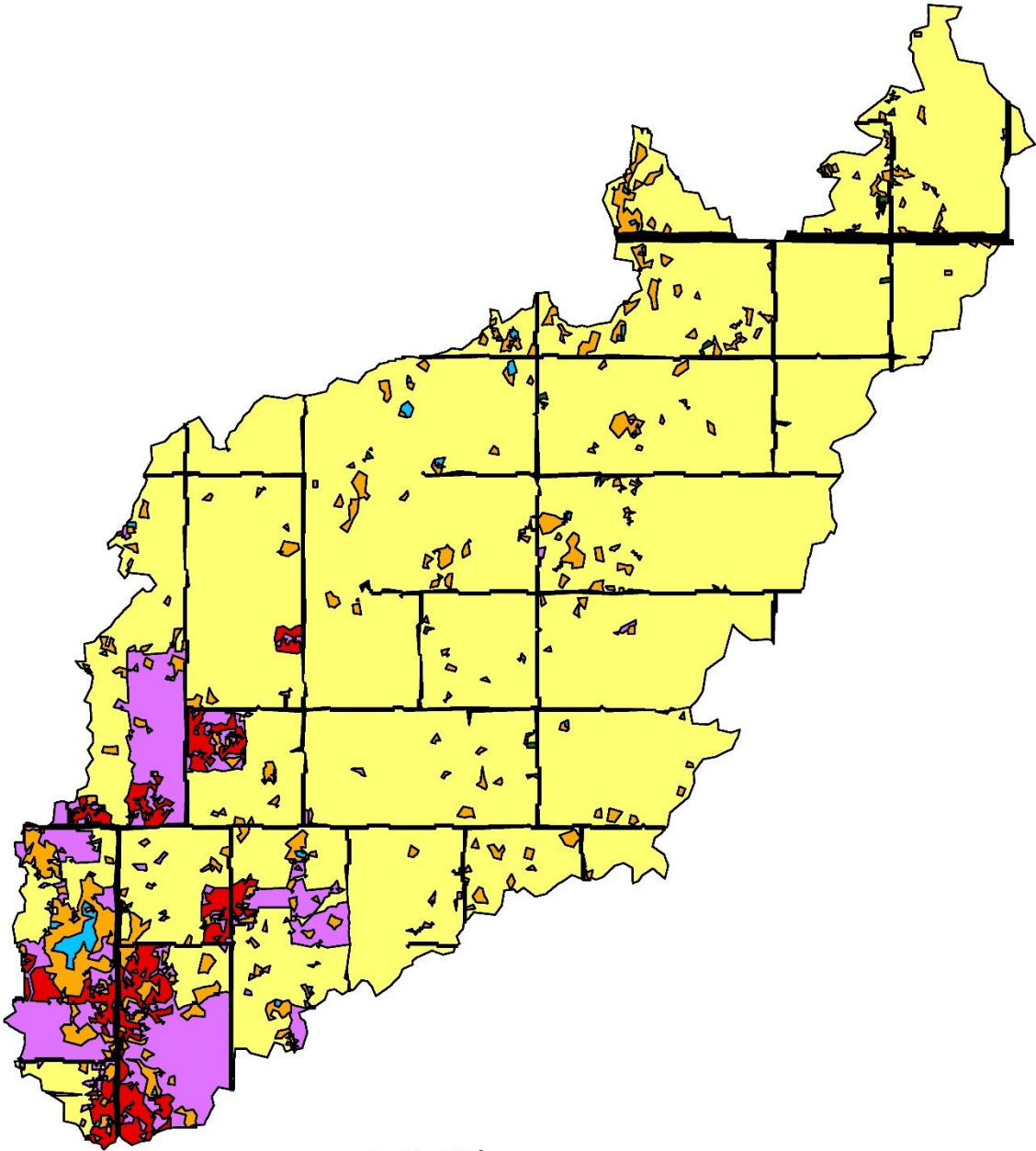
Sub-basin 5

0　　　　　　　　　　　　　9.5 Kilometers

Sub-basin 6

68

0   6.5 Kilometers

Sub-basin 7

0   10 Kilometers

Sub-basin 8
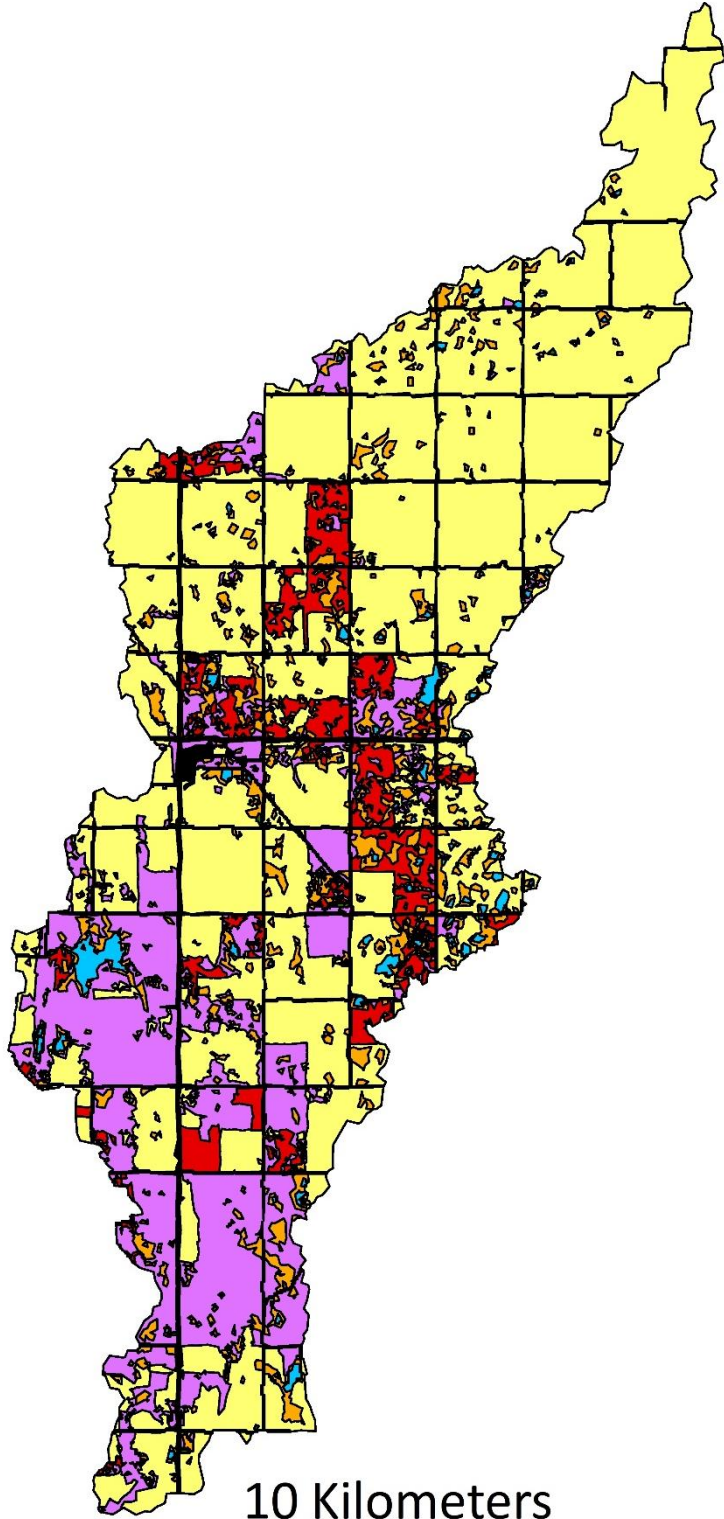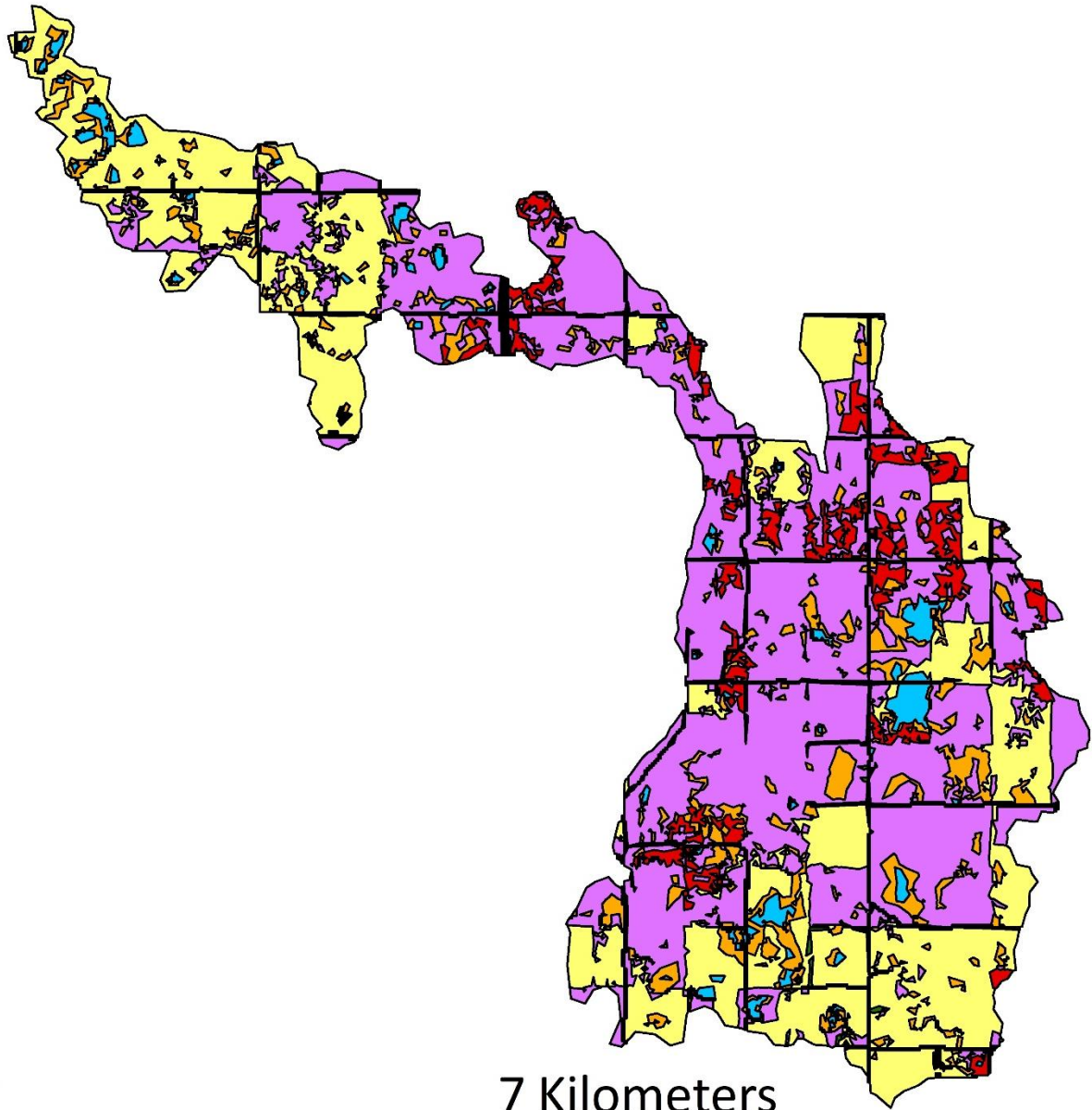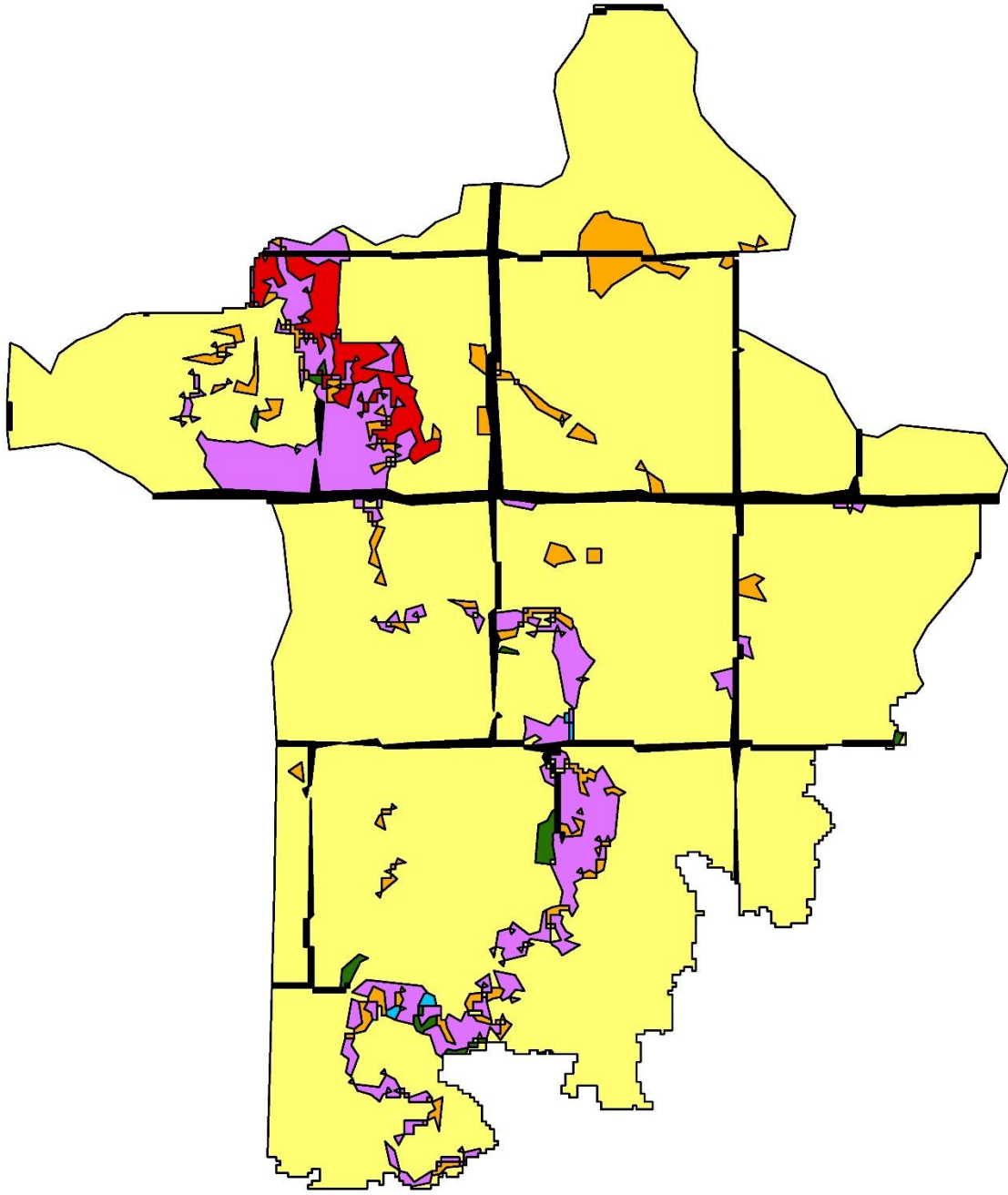
0   7 Kilometers

Sub-basin 9

0   3 Kilometers

Sub-basin 10

Appendix B

Model Setup Files

USB Drive (E:)/CRHM

REFERENCES

Ahmari, H., Blais, E. L., & Greshuk, J. (2016). The 2014 flood event in the Assiniboine River Basin: Causes, assessment and damage. *Canadian Water Resources Journal*, *41*(1-2), 85-93.

Annandale, J., Jovanovic, N., Benadé, N., & Allen, R. (2002). Software for missing data error analysis of Penman-Monteith reference ET. *Irrigation Science, 21*(2), 57-67.

Ayers, H. D. (1959). Influence of soil profile and vegetation characteristics on net rainfall supply to runoff. Proceedings from: *Hydrology Symposium No.1 Spillway Design Floods: Vol. 1*. (pp. 198-205). Ottowa, ON: National Research Council Canada.

Bassler, R. (2010). Metadata Summary. Retrieved from http://lidar.swc.nd.gov/

Blais, E. L., Greshuk, J., & Stadnyk, T. (2016). The 2011 flood event in the Assiniboine River Basin: Causes, assessment and damages. *Canadian Water Resources Journal, 41*(1-2), 74-84.

Bluemle, J. (2003). Generalized Bedrock Geologic Map of North Dakota [map]. Miscellaneous Map Series, map MM-36. North Dakota Geological Survey.

Bluemle, J. (2005). North Dakota's Mountainous Areas: The Killdeer Mountains and Turtle Mountains. In *North Dakota Notes* (15). Retrieved from https://www.dmr.nd.gov/ndgs/ndnotes/ndn15-h.htm

Bonsal, B. R., Wheaton, E. E., Chipanshi, A. C., Lin, C., Sauchyn, D. J., & Wen, L. (2011). Drought research in Canada: a review. *Atmosphere-Ocean, 49*(4), 303-319.

Bonsal, B. R., Aider, R., Gachon, P., & Lapp, S. (2013). An assessment of Canadian prairie drought: past, present, and future. *Climate Dynamics, 41*(2), 501-516.

Bonsal, B. R., Cuell, C., Wheaton, E., Sauchyn, D. J., & Barrow, E. (2017). An assessment of historical and projected future hydro-climatic variability and extremes over southern watersheds in the Canadian Prairies. *International Journal of Climatology, 37*(10), 3934-3948.

Brunt, D. (1932). Notes on radiation in the atmosphere. I. *Quarterly Journal of the Royal Meteorological Society*, *58*(247), 389-420.

Brutsaert, W. (1982). *Evaporation into the Atmosphere.* London, UK: D. Reidel Publishing Company.

Centre for Hydrology, University of Saskatchewan, National Water Research Institute, & Rowan Systems. (2016). The Cold Regions Hydrological Modeling Platform [Software Manual]. Saskatechewan, SK: Author.

Chakaravarti, A. K. (1976). Precipitation deficiency patterns in the Prairie Provinces of Canada. *Prairie Forum–The Journal of the Canadian Plains Research Centre*, *1*, 95-110.

Climate Prediction Center Internet Team. (2012). Pacific/North American. In *Northern Hemisphere Teleconnection Patterns.* Retrieved from http://www.cpc.ncep.noaa.gov/data/teledoc/pna.shtml

Climate Prediction Center Internet Team. (2017). El Niño and La Niña-related winter features over North America. In *The ENSO Cycle*. Retrieved from http://www.cpc.ncep.noaa.gov/products/analysis_monitoring/ensocycle/nawinter.shtml

Coles, A. E., Appels, W. M., McConkey, B. G., & McDonnell, J. J. (2016). *The hierarchy of controls on snowmelt–runoff generation over seasonally-frozen hillslopes*. Manuscript submitted for publication.

Collins, M., Knutti, R., Arblaster, J., Dufresne, J. L., Fichefet, T., Friedlingstein, P., ... & Shongwe, M. (2013). *Long-term climate change: projections, commitments and irreversibility* (Fifth Assessment Report of the Intergovernmental Panel on Climate Change). Cambridge, UK and New York NY: Cambridge University Press.

Cordeiro, M. R., Wilson, H. F., Vanrobaeys, J., Pomeroy, J. W., & Fang, X. (2017). Simulating cold-region hydrology in an intensively drained agricultural watershed in Manitoba, Canada, using the Cold Regions Hydrological Model. *Hydrology and Earth System Sciences, 21*(7), 3483-3506.

Corriveau, J., Chambers, P. A., & Culp, J. M. (2013). Seasonal variation in nutrient export along streams in the Northern Great Plains. *Water, Air, & Soil Pollution, 224*(7), 1594.

Dai, S., Shulski, M. D., Hubbard, K. G., & Takle, E. S. (2016). A spatiotemporal analysis of Midwest US temperature and precipitation trends during the growing season from 1980 to 2013. *International Journal of Climatology, 36*(1), 517-525.

Daly, C., Gibson, W. P., Taylor, G. H., Johnson, G. L., & Pasteris, P. (2002). A knowledge-based approach to the statistical mapping of climate. *Climate Research*, *22*(2), 99-113.

Daly, C., Halbleib, M., Smith, J. I., Gibson, W. P., Doggett, M. K., Taylor, G. H., ... & Pasteris, P. P. (2008). Physiographically sensitive mapping of climatological temperature and precipitation across the conterminous United States. *International Journal of Climatology, 28*(15), 2031-2064.

Dey, B. (1977). Nature and possible causes of heavy summer precipitation in the Canadian Prairies. *Geographical. Perspectives*, *40*, 26-33.

Dey, B. (1982). Nature and possible causes of droughts on the Canadian Prairies-case studies. *International Journal of Climatology*, *2*(3), 233-249.

Dornes, P. F., Pomeroy, J. W., Pietroniro, A., Carey, S. K., & Quinton, W. L. (2008). Influence of landscape aggregation in modelling snow-cover ablation and snowmelt runoff in a sub-arctic mountainous environment. *Hydrological Sciences Journal*, *53*(4), 725-740.

Dumanski, S., Pomeroy, J. W., & Westbrook, C. J. (2015). Hydrological regime changes in a Canadian Prairie basin. *Hydrological Processes, 29*(18), 3893-3904.

Ellis, C. R., & Pomeroy, J. W. (2007). Estimating sub-canopy shortwave irradiance to melting snow on forested slopes. *Hydrological Processes*, *21*(19), 2581-2593.

Ellis, C. R., Pomeroy, J. W., Brown, T., & MacDonald, J. (2010). Simulation of snow accumulation and melt in needleleaf forest environments. *Hydrology and Earth System Sciences*, *14*(6), 925.

Environment and Climate Change Canada. (2018). Glossary. In *About the Data.* Retrieved from http://climate.weather.gc.ca/glossary_e.html

Environment and Climate Change Canada. (2018). *Historical Climate Data* [Data file]. Retrieved from http://climate.weather.gc.ca/historical_data/search_historic_data_e.html

Fang, X., & Pomeroy, J. W. (2007). Snowmelt runoff sensitivity analysis to drought on the Canadian Prairies. *Hydrological Processes, 21*(19), 2594-2609.

Fang, X., & Pomeroy, J. W. (2008). Drought impacts on Canadian prairie wetland snow hydrology. *Hydrological Processes, 22*(15), 2858-2873.

Fang, X., Pomeroy, J. W., Westbrook, C. J., Guo, X., Minke, A. G., & Brown, T. (2010). Prediction of snowmelt derived streamflow in a wetland dominated prairie basin. *Hydrology and Earth System Sciences, 14*(6), 991-1006.

Fang, X., Pomeroy, J. W., Ellis, C. R., MacDonald, M. K., DeBeer, C. M., & Brown, T. (2013). Multi-variable evaluation of hydrological model predictions for a headwater basin in the Canadian Rocky Mountains. *Hydrology and Earth System Sciences, 17*(4), 1635-1659.

Garnier, B. J., & Ohmura, A. (1970). The evaluation of surface variations in solar radiation income. *Solar Energy, 13*(1), 21-34.

Geo Scientific Ltd. *Federal/McCall/Prairie Snow Samplers* [Brochure]. Retrieved from http://www.geoscientific.com/

Granger, R. J., & Male, D. H. (1978). Melting of a prairie snowpack. *Journal of Applied Meteorology*, *17*(12), 1833-1842.

Granger, R. J., Gray, D. M., & Dyck, G. E. (1984). Snowmelt infiltration to frozen prairie soils. *Canadian Journal of Earth Sciences*, *21*(6), 669-677.

Granger, R.J., & Gray, D.M. (1990). A new radiation model for calculating daily snowmelt in open environments. *Nordic Hydrology*, *21*,217-234.

Grassland. (2018). In *Encyclopædia Britannica online*. Retrieved from
https://kids.britannica.com/students/assembly/view/166438

Gray, D.M., Colbeck, S.C., & Ray, M. (1979). Snow accumulation and distribution. Proceedings from: *Workshop/ Meeting on Modelling Snowcover Runoff.* (pp. 3-33). Hanover, NH: US Army Cold Regions Research and Engineering Laboratory.

Gray, D. M., Landine, P. G., & Granger, R. J. (1985). Simulating infiltration into frozen prairie soils in streamflow models. *Canadian Journal of Earth Sciences*, *22*(3), 464-472.

Gray, D. M., Granger, R. J., & Landine, P. G. (1986). Modelling snowmelt infiltration and runoff in a prairie environment. Proceedings from: *Cold Regions Hydrology.* (pp. 427-438). Bethesda, Maryland: American Water Workers Association.

Gray, D. M., Pomeroy, J. W., & Granger, R. J. (1986). Prairie snowmelt runoff. Proceedings from: *Water Research Themes, Conference Commemorating the Official Opening of the National Hydrology Research Centre.* (pp. 49-68). Saskatoon, SK: Canadian Water Resources Association.

Gray, D. M., & Landine, P. G. (1987). Albedo model for shallow prairie snowcovers. *Canadian Journal of Earth Sciences*, *24*(9), 1760-1768.

Gray, D. M., & Landine, P. G. (1988). An energy-budget snowmelt model for the Canadian Prairies. *Canadian Journal of Earth Sciences*, *25*(8), 1292-1303.

Hayashi, M., Van der Kamp, G., & Rudolph, D. L. (1998). Mass transfer processes between a prairie pothole and adjacent uplands, 2: chloride cycle. *Journal of Hydrology*, *207*, 56-67.

Hoerling, M., Eischeid, J., Easterling, D., Peterson, T., & Webb, R., (2010). *Understanding and explaining hydro-climate variations at Devils Lake* (NOAA Publication).

Jarvis, P. G. (1976). The interpretation of the variations in leaf water potential and stomatal conductance found in canopies in the field. *Philosophical Transactions of the Royal Society of London B*, *273*(927), 593-610.

Kharel, G., Zheng, H., & Kirilenko, A. (2016). Can land-use change mitigate long-term flood risks in the Prairie Pothole Region? The case of Devils Lake, North Dakota, USA. *Regional Environmental Change, 16*(8), 2443-2456.

Kluver, D., & Leathers, D. (2015). Winter snowfall prediction in the United States using multiple discriminant analysis. *International Journal of Climatology, 35*(8), 2003-2018.

Krogh, S. A., Pomeroy, J. W., & Marsh, P. (2017). Diagnosis of the hydrology of a small Arctic basin at the tundra-taiga transition using a physically based hydrological model. *Journal of Hydrology, 550*, 685-703.

Lim, Y. H., Hassell, J., & Teng, W. (2010). Modeling hydrologic regime of a Terminal Lake Basin with GCM down-scaled scenarios. Proceedings from: *5th International Congress on Environmental Modelling and Software*. Provo, UT: Brigham Young University.

Liu, J., Stewart, R. E., & Szeto, K. K. (2004). Moisture transport and other hydrometeorological features associated with the severe 2000/01 drought over the western and central Canadian Prairies. *Journal of Climate*, *17*(2), 305-319.

López-Moreno, J. I., Pomeroy, J. W., Revuelto, J., & Vicente-Serrano, S. M. (2013). Response of snow processes to climate change: spatial variability in a small basin in the Spanish Pyrenees. *Hydrological Processes, 27*(18), 2637-2650.

Mahmood, T. H., Pomeroy, J. W., Wheater, H. S., & Baulch, H. M. (2017). Hydrological responses to climatic variability in a cold agricultural region. *Hydrological Processes, 31*(4), 854-870.

Masud, M. B., Khaliq, M. N., & Wheater, H. S. (2016). Projected changes to short-and long-duration precipitation extremes over the Canadian Prairie Provinces. *Climate Dynamics*, *49*(5-6), 1597-1616.

McCullough, G. K., Page, S. J., Hesslein, R. H., Stainton, M. P., Kling, H. J., Salki, A. G., & Barber, D. G. (2012). Hydrological forcing of a recent trophic surge in Lake Winnipeg. *Journal of Great Lakes Research*, *38*, 95-105.

Melesse, A. M., Nangia, V., & Wang, X. (2006). Hydrology and Water Balance of Devils Lake Basin: Part 2-Grid-Based Spatial Surface Water Balance Modeling. *Journal of Spatial Hydrology, 6*(1), 133-144.

Mladjic, B., Sushama, L., Khaliq, M. N., Laprise, R., Caya, D., & Roy, R. (2011). Canadian RCM projected changes to extreme precipitation characteristics over Canada. *Journal of Climate*, *24*(10), 2565-2584.

Monteith, J. L. (1965). Evaporation and environment. Proceedings from: *Symposia of the Society for Experimental Biology*: *Vol. 19*. (pp. 205-224).

Motovilov, Y. G. (1978). Mathematical model of water infiltration into frozen soils. *Soviet Hydrology*, *17*(2), 62-66.

Motovilov, Y. G. (1979). Simulation of meltwater losses through infiltration into soil. *Soviet Hydrology*, *18*(3), 217-221.

Multi-Resolution Land Characteristics Consortium. (2006). *National Land Cover* [Data file]. Retrieved from https://www.mrlc.gov/nlcd06_data.php

Munna, H. S. (2012). *Water level quantiles of Devils Lake under down-scaled GCM predictions using a coupled hydro-climatic model* (Master's Thesis). Retrieved from Proquest Digital Dissertations. (AAT 1520095)

Nachshon, U., Ireson, A., van der Kamp, G., & Wheater, H. (2013). Sulfate salt dynamics in the glaciated plains of North America. *Journal of Hydrology*, *499*, 188-199.

Nash, J. E., & Sutcliffe, J. V. (1970). River flow forecasting through conceptual models part I—A discussion of principles. *Journal of Hydrology*, *10*(3), 282-290.

National Resources Conservation Service. (2007). *Devils Lake: 09020201 8-Digit Hydrologic Unit Profile.* (U.S. Department of Agriculture Publication). Bismarck, ND: Autor. Retrieved from <https://www.nrcs.usda.gov/Internet/FSE_DOCUMENTS/nrcs141p2_000795.pdf>.

Red River Mapping Initiative of the International Water Institute. (2010). *LiDAR* [Data file]. Retrieved from http://lidar.swc.nd.gov/.

Perlman, Howard. (2016) How Streamflow is Measured Part 3: The Stage-Discharge Relation. In *The USGS Water Science School*. Retrieved from https://water.usgs.gov/edu/streamflow3.html

Pomeroy, J. W., & Gray, D. M. (1995). *Snowcover-accumulation, relocation and management* (Science Report No. 7) Sakatoon, SK: National Hydrology Research Institute.

Pomeroy, J. W., Hedstrom, N., & Parviainen, J. (1999). The snow mass balance of Wolf Creek, Yukon: effects of snow sublimation and redistribution. Proceedings from: *Wolf Creek, Research Basin: Hydrology, Ecology, Environment Workshop.* (pp. 15-30). Saskatoon, SK: National Water Research Institute & Minister of Environment.

Pomeroy, J. W., Gray, D. M., Brown, T., Hedstrom, N. R., Quinton, W. L., Granger, R. J., & Carey, S. K. (2007). The cold regions hydrological model: a platform for basing process representation and model structure on physical evidence. *Hydrological Processes*, *21*(19), 2650-2667.

Pomeroy, J. W., Marks, D., Link, T., Ellis, C., Hardy, J., Rowlands, A., & Granger, R. (2009). The impact of coniferous forest temperature on incoming longwave radiation to melting snow. *Hydrological Processes*, *23*(17), 2513-2525.

Pomeroy, J. W., Fang, X., & Marks, D. G. (2016). The cold rain-on-snow event of June 2013 in the Canadian Rockies—characteristics and diagnosis. *Hydrological Processes*, *30*(17), 2899-2914.

Popov, E. G. (1973). Snowmelt runoff forecasts—theoretical problems. Proceedings from: *The Banff Symposium: International Symposium on the Role of Snow and Ice in Hydrology*. (pp. 829-839).

Priestley, C. H. B., & Taylor, R. J. (1972). On the assessment of surface heat flux and evaporation using large-scale parameters. *Monthly Weather Review*, *100*(2), 81-92.

PRISM Climate Group, Oregon State University. (2017). *Recent Years Precipitation* [Data file]. Retrieved from http://www.prism.oregonstate.edu/explorer/

Pusc, S. W. (1993). *The Interaction between Ground Water and a Large Terminal Lake Devils Lake, North Dakota: Hydrogeology of the Devils Lake Area*. (Water Resources Investigation No. 13). Bismarck: North Dakota State Water Commission.

Rasouli, K., Pomeroy, J. W., Janowicz, J. R., Carey, S. K., & Williams, T. J. (2014). Hydrological sensitivity of a northern mountain basin to climate change. *Hydrological Processes, 28*(14), 4191-4208.

Rithchison, D., Mullins, B., & Hyde, J. North Dakota Agricultural Network, School of Natural Resource Sciences, North Dakota State University. (2017). *Hourly Weather Data* [Data file]. Retrieved from https://ndawn.ndsu.nodak.edu/weather-data-hourly.html

Rithchison, D., Mullins, B., & Hyde, J. (2018). Variable Definitions. In *Data Information.*. Retrieved from https://ndawn.ndsu.nodak.edu/help-data.html#vrh

Ryan, G. L., & Wiche, G. J. (1988). *Hydrology of the Chain of Lakes tributary to Devils Lake and water-level simulations of Devils Lake, northeastern North Dakota*. (U.S. Geological Survey Water Resources Investigations Report No. 88-4020). Denver, CO: U.S. Geological Survey.

Ryberg, K. R., Akyüz, F. A., Wiche, G. J., & Lin, W. (2016). Changes in seasonality and timing of peak streamflow in snow and semi-arid climates of the north-central United States, 1910–2012. *Hydrological Processes, 30*(8), 1208-1218.

Sankarasubramanian, A., & Vogel, R. M. (2003). Hydroclimatology of the continental United States. *Geophysical Research Letters, 30*(7).

Shabbar, A., Bonsal, B. R., & Szeto, K. (2011). Atmospheric and oceanic variability associated with growing season droughts and pluvials on the Canadian Prairies. *Atmosphere-Ocean*, *49*(4), 339-355.

Shapley, M. D., Johnson, W. C., Engstrom, D. R., & Osterkamp, W. R. (2005). Late-Holocene flooding and drought in the Northern Great Plains, USA, reconstructed from tree rings, lake sediments and ancient shorelines. *The Holocene*, *15*(1), 29-41.

Shook, K., & Pomeroy, J. (2012). Changes in the hydrological character of rainfall on the Canadian Prairies. *Hydrological Processes, 26*(12), 1752-1766.

Shook, K. (2016). The 2005 flood events in the Saskatchewan River Basin: Causes, assessment and damages. *Canadian Water Resources Journal, 41*(1-2), 94-104.

Shuttleworth, W. J. (2012). *Terrestrial hydrometeorology*. West Sussex, UK: John Wiley & Sons.

Sicart, J. E., Pomeroy, J. W., Essery, R. L. H., & Bewley, D. (2006). Incoming longwave radiation to melting snow: observations, sensitivity and estimation in northern environments. *Hydrological Processes, 20*(17), 3697-3708.

Sivapalan, M. (2018). From engineering hydrology to Earth system science: milestones in the transformation of hydrologic science. *Hydrology and Earth System Sciences, 22*(3), 1665.

Small, D., Islam, S., & Vogel, R. M. (2006). Trends in precipitation and streamflow in the eastern US: Paradox or perception?. *Geophysical research letters, 33*(3).

Soil Survey Staff. Natural Resources Conservation Service, U.S. Department of Agriculture. (2016). *Soil Survey Geographic Database* [Data File]. Retrieved from http://resources.arcgis.com/en/communities/soils/02ms0000000n000000.htm

Stadnyk, T., Dow, K., Wazney, L., & Blais, E. L. (2016). The 2011 flood event in the Red River Basin: Causes, assessment and damages. *Canadian Water Resources Journal, 41*(1-2), 65-73.

Sweeney, J. (1985). The 1984 drought on the Canadian Prairies. *Weather, 40*(10), 302-309.

Thomas, H.E. (1962). *The Meteorologic Phenomenon of Drought in the Southwest*. (U.S. Geological Survey Professional Paper No. 342A) Washington, DC: U.S. Geological Survey.

Todhunter, P. E., & Rundquist, B. C. (2008). Pervasive wetland flooding in the glacial drift prairie of North Dakota (USA). *Natural Hazards, 46*(1), 73-88.

Todhunter, P. E. (2016). Mean hydroclimatic and hydrological conditions during two climatic modes in the Devils Lake Basin, North Dakota (USA). *Lakes & Reservoirs: Research & Management, 21*(4), 338-350.

Todhunter, P. E., & Fietzek-DeVries, R. (2016). Natural hydroclimatic forcing of historical lake volume fluctuations at Devils Lake, North Dakota (USA). *Natural Hazards, 81*(3), 1515-1532.

Trenberth, K. E. (2011). Changes in precipitation with climate change. *Climate Research*, *47*(1/2), 123-138.

U.S. Department of Agriculture Farm Service Agency Aerial Photography Field Office. (2017). *Color Infrared* [Data File]. Retrieved from https://ndgishub.nd.gov/arcgis/rest/services/Imagery/AerialImage_ND_2017_CIR/ImageServer

U.S. Environmental Protection Agency, North Dakota State Department of Health- Division of Water Quality, South Dakota State Department of Environment and Natural Resources, South Dakota State University- Department of Wildlife and Fisheries Sciences, the U.S Forest Service, Natural Resources Conservation Service, & U.S. Geological Survey. (1998). Ecoregions of North and South Dakota [map]. Authors.

U.S. Geological Survey. (2017). *Discharge* [Data File]. Retrieved from https://waterdata.usgs.gov/nwis/uv?05056100

U.S. Geological Survey (2017). *National Hydrography Dataset* [Data File]. Retrieved from http://nhd.usgs.gov/index.html

Vandeberg, G. S., Dixon, C. S., Vose, B., & Fisher, M. R. (2015). Spatial assessment of water quality in the vicinity of Lake Alice National Wildlife Refuge, Upper Devils Lake Basin, North Dakota. *Environmental Monitoring and Assessment, 187*(2), 40.

Vecchia, A. V. (2002). *Simulation of a proposed emergency outlet from Devils Lake, North Dakota*. (U.S. Geological Survey Water Resources Investigations Report No. 02-4042). Denver, CO: U.S. Geological Survey.

Vecchia, A. V. (2008). *Climate simulation and flood risk analysis for 2008-40 for Devils Lake, North Dakota*. (U.S. Geological Survey Scientific Investigations Report No. 2008-5011). Denver, CO: U.S. Geological Survey.

Verseghy, D. L. (1991). CLASS—A Canadian land surface scheme for GCMs. I. Soil model. *International Journal of Climatology, 11*(2), 111-133.

Weakly, H. E. (1943). A tree-ring record of precipitation in western Nebraska. *Journal of Forestry, 41*(11), 816-819.

Wiche, G.J., & Pusc, S.W. (1994) *Hydrology of Devils Lake area, North Dakota* (North Dakota State Water Commission Water Resources Investigations Report No. 22). Bismarck, North Dakota: U.S. Geological Survey.

Wiche, G.J., Vecchia, A.V., Osborne, L., & Fay, J.T. (2000). *Climatology and potential effects of an emergency outlet, Devils Lake Basin, North Dakota* [Fact sheet]. Retrieved from https://pubs.usgs.gov/fs/2000/0089/report.pdf

Zhang, X. (2010). The Fate of Devils Lake: An Interwoven Aftermath of Agriculture and Climate Change. Proceedings from: *5th International Congress on Environmental Modelling and Software*. Provo, UT: Brigham Young University.